QUANTITATIVE ASSESSMENT OF WRIST RIGIDITY IN PARKINSON'S DISEASE BY USING BUILT-IN SENSORS OF A SMARTPHONE

by

Uğur Dinçer

B.S., Mechanical Engineering, Doğuş University, 2014

Submitted to the Institute for Graduate Studies in
Science and Engineering in partial fulfillment of
the requirements for the degree of
Master of Science

Graduate Program in Mechanical Engineering
Boğaziçi University

2020

ACKNOWLEDGEMENTS

I want to especially thank my advisor Prof. Evren Samur and my co-advisor Prof. Çetin Yılmaz for their help and support throughout my study. It would not be possible to complete my thesis without the guidance of them. I would also like to thank Assist. Prof. Sinan Öncü, Assist. Prof. İ. Faik Başkaya and Assist. Prof. İ. Fatma Nazlı Durmaz Çelik accepting to be jury members of my thesis regardless of their busy schedule.

I am especially grateful to Prof. Dr. Muhittin Cenk Akbostancı from Ankara University Faculty of Medicine Department of Neurology, and the neurologists from the same department: Rezzak Yılmaz, Sabiha Tezcan Aydemir, Yasemin Ünal and Turgut Şahin for their cooperation and supports.

I sincerely thank my friend and study partner Günay Züngör for his patience and endurance during the study, also for his valuable and farsighted ideas. Also, I am especially grateful to my friends from Haptics and Robotics Laboratory: Serhat Demirtaş, Bora Baydere, Şeref Kemal Talaş, Taylan Atakuru, Burcu Seyidoğlu, Kübra Karacan, and Haluk Kundakçıoğlu.

Finally, my special thanks go to my wife Bircan and my parents Şerife and Hayri Dinçer for their precious love, supports and inspirations which have made this thesis possible.

ABSTRACT

QUANTITATIVE ASSESSMENT OF WRIST RIGIDITY IN PARKINSON'S DISEASE BY USING BUILT-IN SENSORS OF A SMARTPHONE

Rigidity is one of the motor symptoms of Parkinson's Disease (PD) which is described as an increased muscle tone that occurs throughout the entire range of motion of a limb. Clinical assessment of rigidity is highly subjective; it depends on the experience of the examiner. In this thesis, wrist rigidity is evaluated numerically by using data obtained from the accelerometer, gyroscope and capacitive touch screen of a smartphone. Due to lack of a built-in force sensor, a novel gadget has been developed to be used as a force sensor on the phone screen. The gadget is calibrated to convert the number of pixels to force values. Subsequently, a set of experiments were performed to measure rigidity with the phone. Totally, 11 healthy and 10 PD patients participated in the clinical experiments. Rigidity measurements were performed on the right wrist of the subjects, and scores were assessed according to the Unified Parkinson's Disease Rating Scale (UPDRS) obtained by neurologists before the clinical trials. Experiments were conducted with and without a contralateral hand movement (Froment's Maneuver). In addition, the experiments were conducted in "on" and "off" conditions. "On" condition refers the improvement of symptoms by the administration of anti-parkinsonian medications, "off" condition refers the aggravation of symptoms due to withdrawal of medications. The results have shown that the method can assess the severity of wrist rigidity according to the UPDRS rigidity scale in a confidence interval of 95%. The rigidity scores of the patients in the "off" condition were found higher than the "on" condition ($\alpha = 0.05$). In addition, performing a contralateral hand maneuver aggravated the rigidity ($\alpha = 0.05$). Considering the results, the method can be adopted clinically to assess rigidity.

ÖZET

PARKİNSON HASTALIĞINDAKİ BİLEK SERTLİĞİNİN BİR AKILLI TELEFONUN BÜTÜNLEŞİK SENSÖRLERİNİN KULLANILARAK SAYISAL OLARAK DEĞERLENDİRİLMESİ

Parkinson hastalığının motor semptomlarından birisi olan rijidite, bir uzvun tüm hareket aralığı boyunca görülen artmış kas tonusu olarak tanımlanmaktadır. Rijiditenin klinik olarak derecelendirilmesi, değerlendiren kişinin tecrübesine bağlı olduğu için oldukça özneldir. Bu çalışmada, bilek rijiditesi bir akıllı telefonun ivmeölçer, jiroskop ve kapasitif dokunma ekranından elde edilen veriler kullanılarak sayısal olarak değerlendirilmiştir. Genel olarak günümüz telefonlarında bütünleşik bir kuvvet sensörü olmadığı için, telefonun ekranında kuvvet sensörü olarak kullanılmak üzere bir aparat geliştirilmiştir. Aparatın telefon ekranında etkileşime girdiği piksel sayısını, kuvvet bilgisine dönüştürmek için bir kalibrasyon işlemi yapılmıştır. Daha sonra bir akıllı telefon ile rijidite ölçümü için bir dizi deneyler yaplmıştır. Yapılan klinik deneylere toplamda 11 sağlıklı, 10 Parkinson hastası katılmıştır. Rijidite ölçümleri deneye katılan bireylerin sağ el bileğinde yapılmıştır. Hastaların rijidite değerleri Birleşik Parkinson Hastalığı Değerleme Ölçeği 'ne (BPHDÖ) göre deneylerden önce nörologlar tarafından değerlendirilmiştir. Deneyler hastanın Froment manevrası yaptığı ve yapmadığı durumlar için tekrarlanmıştır. Ek olarak, deneysel metot ve prosedür hastanın ilaç sonrası rijiditesindeki değişimi görmek için genişletilmiştir. Elde edilen sonuçlar metodun hastaların rijidite derecesinin değerlendirilmesinde %95 güven aralığı ile kullanılabileceğini göstermiştir. Froment manevrasının yapıldığı ve hastaların Parkinson karşıtı ilaçları kullanmadıkları deneylerde bulunan rijidite değerleri daha yüksek bulunmuştur ($\alpha = 0.05$). Sonuçlar göz önünde bulundurulduğunda, önerilen metot klinik olarak rijiditenin değerlendirilmesinde kullanılabilir.

TABLE OF CONTENTS

ACKNOWLEDGEMENTS i
ABSTRACT ii
ÖZET iii
LIST OF FIGURES vi
LIST OF TABLES xi
LIST OF SYMBOLS xiii
LIST OF ACRONYMS/ABBREVIATIONS xiv
1. INTRODUCTION 1
1.1. Background 1
1.1.1. Rigidity in Parkinson's Disease 1
1.1.2. Clinical Scales 2
1.1.2.1. Hoehn and Yahr Scale 2
1.1.2.2. Unified Parkinson's Disease Rating Scale 2
1.1.3. Froment Maneuver 3
1.1.4. Deep Brain Stimulation 4
1.1.5. "On" and "Off" Periods in Parkinson's Disease 5
1.2. Motivation 5
1.3. Objectives of the Study 6
2. LITERATURE REVIEW 7
3. MATERIALS AND METHODS 16
3.1. Using Built-in Sensors of a Smartphone 16
3.1.1. Angle Detection 17
3.1.2. Force Sensing Using Capacitive Touch Screen 18
3.1.2.1. Information About Registered Touch Events 18
3.1.2.2. Design and Manufacturing of a Touch Gadget 19
3.1.2.3. Calibration of the Gadget 21
3.1.3. Developed Smartphone Application 21
3.1.4. Remote File Transfer Server for Data Storage 25
3.2. Experimental Methods 25

3.2.1. Procedure 25
3.2.1.1. Froment Maneuvers Performed in the Trials 29
3.2.1.2. Randomization of Experimental Trials 31
3.2.2. Subjects 32
3.2.3. Calculation of Elastic Stiffness 32
4. RESULTS AND DISCUSSION 35
4.1. Calibration Results 35
4.2. Rigidity Measurement Results 38
5. CONCLUSION 52
5.1. Contributions and Originality 53
5.2. Outlook and Future Work 53
REFERENCES 54
APPENDIX A: TECHNICAL DRAWINGS 57
APPENDIX B: FORMS 60

LIST OF FIGURES

Figure 1.1. The stiff wrist test (reprinted from [8]). 4

Figure 1.2. (a) Programmable signal generator, (b) electrodes after implementation front view, (c) electrodes after implementation side view (reprinted from [9]). 5

Figure 2.1. Experimental setup for recording EMG signal while the wrist being flexed and extended with contralateral activation maneuver (reprinted from [10]). 7

Figure 2.2. The apparatus used by Wright and Johns [11]. A: cable, B: pulley converting motion to sinusoidal rotation, C : lever, D: swivel, E: holder, F : center indicator (reprinted from [11]). 8

Figure 2.3. Linear regression analyze of biceps long latency response and instrumental rigidity performed by Webster and Mortimer [12] (reprinted from [12]). 9

Figure 2.4. Schematic view of the apparatus used by Teräväinen *et al.* [13] AC : adjustable rubbers, AR: arm rest, MS: motor shaft, HD: handle, C: controller, TM: torque motor (reprinted from [13]). 10

Figure 2.5. Transducer used by Caligiuri [14] to assess wrist rigidity. A: force gauge, B: rotation encoder (reprinted from [14]). 11

Figure 2.6. The use of the device to assess elbow and wrist rigidity designed by Patrick *et al.* [16]. The position of the device and forearm is different to assess wrist rigidity (not shown in the figure, reprinted from [16]). 12

Figure 2.7. Relationship between measured mechanical impedance values and clinical rigidity scores of the subjects (reprinted from [16]). 13

Figure 2.8. The use of the device designed by Park *et al.* [17] (reprinted from [17]). 14

Figure 3.1. Global and device coordinate systems (reprinted from [20]). 16

Figure 3.2. Schematic explanation of balance filter (reprinted from [20]). . . . 18

Figure 3.3. Exploded 3D model of the designed touch gadget: (a) and (b) isometric views, (c) side view. 19

Figure 3.4. The manufactured touch gadget to convert capacitive touch sensor output to force: (a): back of the gadget where the force is applied, (b): front of the gadget touching the phone screen. 20

Figure 3.5. The schematic presentation of the calibration process. A: parallel beam mechanism, B: force sensor. 21

Figure 3.6. Screenshots of the designed application: (a) main screen, (b) configuration screen. 22

Figure 3.7. After the first touch occurred on the screen, the application starts to collect touch area and orientation of the device: (a) shortly after the touch event registers, (b) the touch event is over. 23

Figure 3.8. UML class diagram of sensor-related clasesses of the application. . 24

Figure 3.9. The forearm posture during the experimental trials: A and B are medical loop straps to fix the forearm to a table, C is an apparatus to fix the smartphone to the hand, D is a case for the phone, E is a chair for subjects to sit, and F is a thin cushion to make the forearm comfortable. 26

Figure 3.10. Rotation of the hand about the wrist by the force applied to the gadget with the right thumb of the operator: (a) the initial position of the loading cycle, (b) and (c) intermediate positions, (d) the final position of the loading cycle. 28

Figure 3.11. The first contralateral activity: (a) the index finger is away from the face, (b) the index finger touches the patient's nose. The subjects were asked to perform this activity periodically. 29

Figure 3.12. The second contralateral activity: (a) the hand is closed, (b) the hand is opened. The subjects were asked to perform this activity periodically. 30

Figure 3.13. Exported angle and force data of PD patient 8. 33

Figure 3.14. Stiffness lines fitted to moment-angle data. 34

Figure 4.1. Data collected from the capacitive touch screen and the force sensor during the calibration process: normalized touch sizes acquired from the smartphone (top), and measured forces (bottom). 35

Figure 4.2. Measured force vs touch sizes. The calibration line is shown with blue solid line. 37

Figure 4.3. Scatter plot of stiffness values according to CRSs. 40

Figure 4.4. Interval bar plots of Tukey's HSD test results. 42

Figure 4.5. Box plots of clinical rigidity groups. 42

Figure 4.6. The stiffness difference between on and off conditions. (a) and (c) are the line plots of individual stiffness values, (b) and (d) are the boxplots of stiffness values. 44

Figure 4.7. The graphical summary of the activated and rest trials. (a) and (c) are the line plots of individual stiffness values, (b) and (d) are the boxplots of the activated and rest trials. 45

Figure 4.8. The graphical summary of the comparison of two trials that the maximum stiffness differences are expected. (a) The line plots of individual stiffness values, (b) the boxplots of the compared groups. 46

Figure 4.9. The graphical summary of the activated and rest trials of the control groups. (a) the line plots of the stiffness values of activated and rest trials, (b) the boxplot of the same trials. 48

Figure 4.10. Interval plots of the control group and PD patients, control subjects who have the sign of rigidity were excluded from the control group. 49

Figure 4.11. Box plots of the control group and PD patients, control subjects who have the sign of rigidity were excluded from the control group. 50

Figure 4.12. Measured elastic coefficients by Endo *et al.* [19], A: extension, B: flexion (reprinted from [19]). 51

Figure 4.13. Relationship between elastic stiffness and UPDRS rigidity score. "-1" indicates healthy controls (reprinted from [17]). 51

Figure A.1. The top cover of the gadget. A: bottom view, B: top view. All dimensions are in mm. 57

Figure A.2. The body of the gadget. A: bottom view, B: top view. All dimensions are in mm. 57

Figure A.3. The molds of the gadget tips. A1: top view of the mold used for the center tip, A2: side view, B1: top view of the molds used for the support tips, B: side view. All dimensions are in mm. 58

Figure A.4. Samsung s10e dimensions. 59

Figure B.1. The informed consent form. 60

Figure B.2. The patient follow-up form. 61

LIST OF TABLES

Table 1.1. Rating scale to describe the progression of PD by Hoehn and Yahr [5]. 2

Table 1.2. Rigidity scale in the UPDRS motor examination section [7]. 3

Table 2.1. Found finger joint stiffness values by Wrigt and Johns [11]. 9

Table 3.1. The table of randomized trials for PD patients and controls. 31

Table 3.2. CRSs of the PD patients and healthy controls. 32

Table 4.1. Linear regression results of each calibration cycle. 36

Table 4.2. Descriptive statistics about the data collected from PD patients. . 39

Table 4.3. Descriptive statistics about the clinical rigidity groups. 40

Table 4.4. Table of Tukey's simultaneous tests for difference of groups means. 41

Table 4.5. Descriptive statistics about the clinical trials. 43

Table 4.6. The median differences between clinical trials. 43

Table 4.7. Descriptive statistics about the data collected from healthy subjects. 47

Table 4.8. Descriptive statistics about the grouped stiffness values evaluated for control subjects. 48

Table 4.9. Table of Dunnett simultaneous tests, comparing PD group means with control mean. 49

LIST OF SYMBOLS

b	Balance filter coefficient
d	Orientation computed from accelerometer and magnetometer sensors
f	Fused orientation
g	Gyroscope values obtained from a sensor
K	Stiffness
M	Moment
Z	Mechanical impedance
Θ	Angle of rotation

LIST OF ACRONYMS/ABBREVIATIONS

ANOVA	Analysis of variance
API	Application Programming Interface
BPHDÖ	Birleşik Parkinson Hastalığı Değerleme Ölçeği
CRS	Clinical Rigidity Score
DBS	Deep Brain Stimulation
FTP	File Transfer Protocol
HY	Hoehn and Yahr
IMU	Inertial Measuring Unit
MRI	Magnetic Resonance Imaging
ORS	Objective Rigidity Score
PD	Parkinson's Disease
STN-HFS	Subthalamic Nucleus
UML	Unified Modelling Language
UPDRS	Unified Parkinson Disease Rating Scale
vCPU	Virtual Central Processing Unit

1. INTRODUCTION

Present chapter introduces the problem in the literature of movement disorders and neurology, then explains the motivation behind this study, and its goals and objectives.

1.1. Background

Parkinsonism or Parkinson's Disease (PD) was first described by James Parkinson in 1871 in his essay on the Shaking Palsy [1]. He characterized symptoms of PD or "The Shaking Palsy" as follows; resting tremor, lessened muscular power, walking gait with involuntary acceleration, and flexed posture. However, Parkinson himself did not focus on the rigidity in PD patients. Current recognition and description of PD were identified over a long period of time, and it is expanded by numerous neurologists since Parkinson's essay on the Shaking Palsy.

1.1.1. Rigidity in Parkinson's Disease

Over 50 years later, Jean-Martin Charcot refined and expanded Parkinson's definition. [2]. Rigidity, altered muscle tone, is characterized by the increased resistance to passive movement of the limb, was explicitly recognized by him, he used the term Parkinson's Disease partially rejecting earlier definition of the Shaking Palsy, because the patients don't necessarily have tremor but having arthrosis/muscular rigidity.

In PD, two types of rigidity can be observed: cogwheel and lead-pipe, these rigidity types may coexist in a PD patient. In the lead-pipe rigidity, the increased muscle tone is uniform and continuous throughout the entire range of the motion of a limb for both flexion and extension movements [3]. On the other hand, cogwheel rigidity is disrupted at a 4 to 6 Hz frequency, and sometimes at 8 to 9 Hz frequency along the range of movement of the limb, rigidity is not uniform and continuous, but rhythmic short increased muscle tone [4].

1.1.2. Clinical Scales

Accurate assessment of the severity of PD is crucial for the treatment. Besides bradykinesia and hand tremor, rigidity is also important because it strongly respond to two treatment methods: dopaminergic medication and deep brain stimulation (DBS). The following two subsections introduce two stating systems for PD: Hoehn and Yahr Scale, and The Unified Parkinson's Disease Rating Scale (UPDRS).

1.1.2.1. Hoehn and Yahr Scale. In 1967, medical doctors Hoehn and Yahr published a study in which they introduced first rating system commonly accepted by neurologist, internationally [5]. They proposed 5 stages as seen in Table 1.1 to describe the progression of PD.

Table 1.1. Rating scale to describe the progression of PD by Hoehn and Yahr [5].

	Corresponding Clinical Severity
Stage I	Unilateral involvement only, minimal or no functional impairment
Stage II	Bilateral or midline involvement, without impairment of balance
Stage III	First sign of impaired righting reflexes
Stage IV	Fully developed, severely disabling disease
Stage V	Confinement to bed or wheelchair unless aided

In time, this scale has been modified with the addition of two more intermediate stages 1.5 and 2.5 due to inadequate stages at the low-level impairment stages. However, Movement Disorder Society Task Force report in 2004 recommended that the HY scale must be used in its original form because no clinometric data are available on modified HY scale [6].

1.1.2.2. Unified Parkinson's Disease Rating Scale. The UPDRS is a set of clinical examinations and questions to assess both motor and non-motor symptoms associated with Parkinson's Disease. The UPDRS is widely accepted by clinicians, internationally.

It consist of four section as follows, section one is about mentation, behavior and mood, section two is about activities of daily living, section three is about motor examination such as rigidity, tremor at rest, postural ability etc., last section is about complications [7]. The clinician assesses the patient quantitatively between 0 (absent) and 4 (severe). The given total UPDRS score to a patient after the examination varies between 0 to 199, high score means the severity of the PD is high. For rigidity the UPDRS scores are given with their clinical descriptions in Table 1.2.

Table 1.2. Rigidity scale in the UPDRS motor examination section [7].

UPDRS Score	**Rigidity**
0	Absent
1	Slight or detectable
2	Mild
3	Marked, however range of motion easily achieved
4	Severe, range of motion achieved with difficulty

1.1.3. Froment Maneuver

French neurologist, Jules Froment [8], researched mostly focusing on how the posture of the body affects the rigidity in PD patients during 1920s. Froment stated that rigidity can be marked more specially and easily when there is a voluntary motion of another limbs as seen in Figure 1.1.

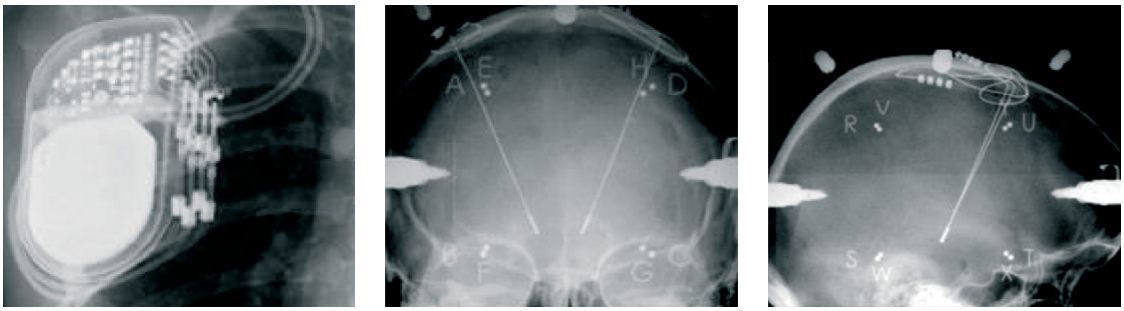
Froment tested this effect with the maneuver that the patient was asked to "swing his arm around like a windmill". This maneuver named as "Froment maneuver" in the medical literature [8]. The Froment maneuver also can be achieved with the contralateral limb movement that is under resistance to the gravity. Froment also showed that when patients at relaxed body position in a comfortable armchair where all body parts supported against gravity forces, the rigidity of the wrist diminishes. In this study, we collected data from each subject in the presence and absence of a contralateral limb movement.



Figure 1.1. The stiff wrist test (reprinted from [8]).

1.1.4. Deep Brain Stimulation

Deep brain stimulation (DBS) is a surgical treatment for advanced PD. It stimulates the subthalamic nucleus (STN-HFS) with high frequency electrical signal, generally at 130 Hz. Magnetic resonance imaging (MRI) and stereotactic ventriculography are used as pre-operative imaging tools to find the best location for electrodes as seen in Figure 1.2. Clinical response to DBS can be monitored during the operation and the success of the operation is measured by decreased severity of the symptoms. Many symptoms of PD can be assessed during the operation because implantation is usually done under local anesthesia. However, assessment of wrist rigidity is more practical than assessing other symptoms because the examiner can assess the wrist by himself just applying flexion and extension movements to the wrist without the patient's participation [9].



(a) (b) (c)

Figure 1.2. (a) Programmable signal generator, (b) electrodes after implementation front view, (c) electrodes after implementation side view (reprinted from [9]).

1.1.5. "On" and "Off" Periods in Parkinson's Disease

"On" and "off" terms are used by clinicians to describe the different stages of the motor fluctuations. In the on period, the symptoms of the disease are controlled with anti-parkinsonian medicines or DBS. On the other hand, off period indicates the condition of withdrawal from dopaminergic medication. In this study, we collected data from each subject for both conditions under the supervision of neurologists.

1.2. Motivation

Monitoring the severity of motor symptoms, deciding at which stage the patient is, and observing the patient's response to treatment are curial for PD. Although, there are two commonly used clinical rating systems which are the UPDRS and Hoehn and Yahr scale, to determine the severity and degree of symptoms, their subjectivity caused them to be constantly questioned. This subjectivity can be more dominant when assessing the rigidity. Numerous studies have tried to solve this problem with developing different methods and devices; however, there is not practical, and accurate method or device, currently. Treatment of the disease may be more effective with observing rigidity more accurately via an easy-to-apply method. This method may replace the subjective assessment of the parkinsonian rigidity.

1.3. Objectives of the Study

This study assumes that the human wrist can be modelled as a mechanical system containing only an elastic component. The elastic component can be found by using built-in sensors of a smartphone: accelerometer, gyroscope, and capacitive touch screen. The main hypothesis of this study is that the elastic component can be used as a sole indicator of the wrist rigidity, and the model parameter can be mapped into UPDRS rigidity scale. The study can be considered to have the following objectives:

Objective 1: Designing, manufacturing, and calibrating a gadget to get applied force to the phone screen. Most of android smartphones have an application programming interface (API) that returns the size of a registered touch event, the size information can be converted to the corresponding force by a simple calibration process. In order to make this pixel-force conversion with high inter- and intra-rater reliability, a gadget having a soft semi-conductor tip is designed.

Objective 2: Designing an experimental setup and developing a procedure for measuring rigidity in both on and off conditions as well as for measurements with and without contralateral hand movements.

Objective 3: Performing an experimental study to prove that the method can be used for assessing wrist rigidity in a clinical environment with confidence interval of %95.

When the above specific objectives are achieved, the method will make the clinical assessment of wrist rigidity more objective, accurate and practical. In addition, the treatment response of patients will be safely and easily monitored. The method just requires a smartphone and a small gadget to assess wrist rigidity, this might make the method to be widely accepted method by neurologists. In fact, we aim that the method will be a standard in clinical rigidity examinations not only for PD but also other movements disorders.

2. LITERATURE REVIEW

In this chapter, previous studies trying to evaluate rigidity are described in the literature. Rigidity assessments in these studies can be categorized into three categories as follows: studies which used inertial sensors, servomotors, and biomechanical and neurophysiological muscle measurement techniques such as electromyography.

One of the earlier studies that investigate parkinsonian rigidity at the wrist was researched by Matsumoto *et al.* [10]. They conducted experiments to classify the wrist rigidity in five grades very similar to the UPDRS rigidity score. Matsumoto et al. evaluated the wrist rigidity applying passive movements to the wrist with and without contralateral voluntary movements to achieve the Froment's maneuver.

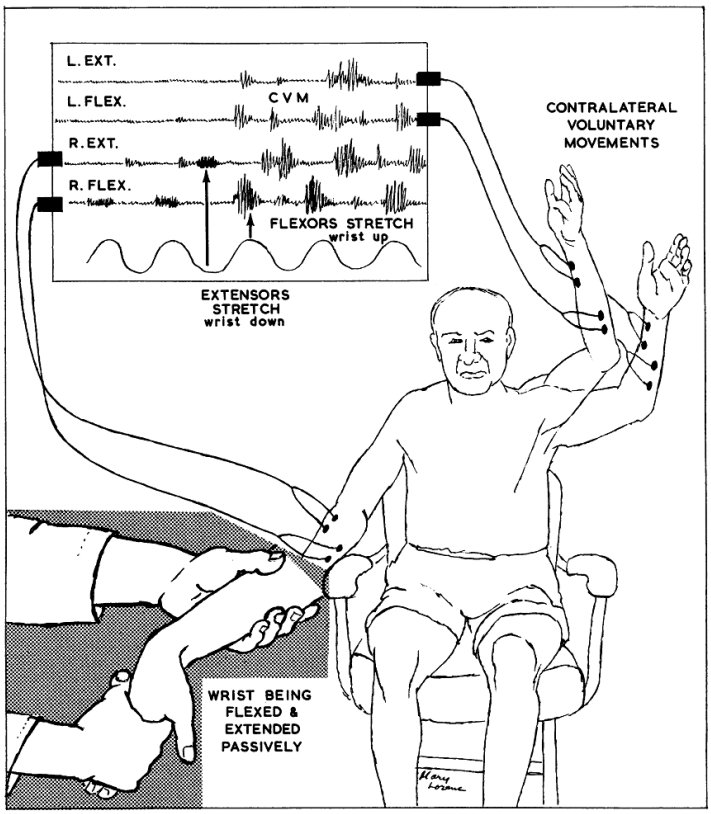


Figure 2.1. Experimental setup for recording EMG signal while the wrist being flexed and extended with contralateral activation maneuver (reprinted from [10]).

They placed surface electrodes of the EMG device on the flexors and extensors muscles of both the wrist of tested arm and contralateral arm. While experiments were conducted, patients were sitting in a comfortable position. Discharges that were caused by stretching of the wrist and voluntary contralateral movements were recorded. They concluded that stretch responses of the wrist can be exaggerated with contralateral voluntary movements while in normal persons no stretch discharge is confirmed with or without contralateral reinforcement. While their findings contributed to understanding parkinsonian rigidity and its mechanisms, they do not correlate the signal indices and rigidity scale of patients.

Wright and Johns [11] researched joint stiffness in physical terms, they investigated finger joints with an apparatus shown in Figure 2.2.

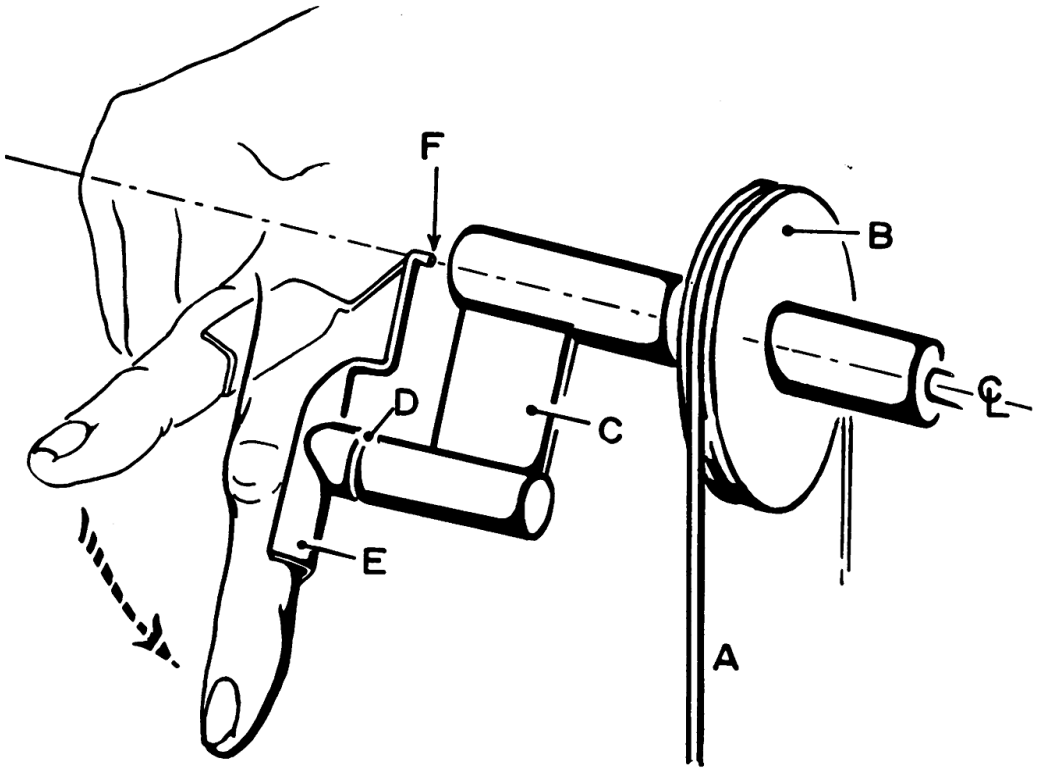


Figure 2.2. The apparatus used by Wright and Johns [11]. A: cable, B: pulley converting motion to sinusoidal rotation, C : lever, D: swivel, E: holder, F : center indicator (reprinted from [11]).

They concluded that elastic stiffness component of the joint model contributes to rigidity more than the viscous component, and the contribution of the frictional and inertial components are negligible. The found stiffness values are given in Table 2.1.

Table 2.1. Found finger joint stiffness values by Wrigt and Johns [11].

Sex	**Stiffness at Flexion [kg.cm/rad]**	**Stiffness at Extension [kg.cm/rad]**
Male	2.31 ± 0.81	2.96 ± 1.30
Female	1.52 ± 0.81	1.70 ± 0.68

Webster and Mortimer [12] examined the relationship between the rigidity and the normalized magnitude of EMG responses. They designed an experimental setup with a servo-controlled device to rotate the forearm through a 100° arc about the elbow. They utilized the net work done by the device integrating the torque over angle to evaluate rigidity. They conducted experiments with and without contralateral activation movements. In Figure 2.3, their relationship between EMG indices and activated rigidity is presented.

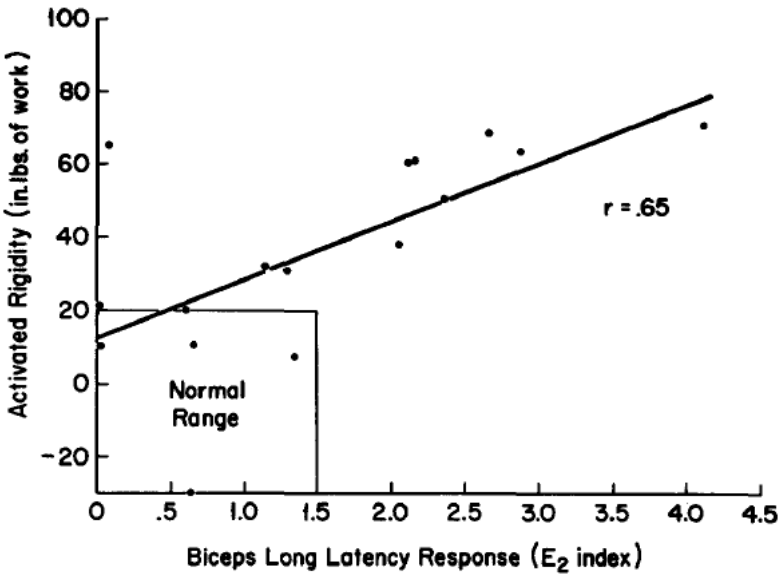


Figure 2.3. Linear regression analyze of biceps long latency response and instrumental rigidity performed by Webster and Mortimer [12] (reprinted from [12]).

Teräväinen *et al.* [13] tried to assess parkinsonian rigidity at the wrist by determining the optimal angular displacement and velocity. They used a torque motor to move the wrist. In addition, a frequency generator was used to generate position signal, the generated signal then fed to a power supply. Schematic view of the apparatus can be seen in Figure 2.4. The area under the torque-angle cycles were calculated and used as the measurement of wrist rigidity. Clinical experiments were conducted with 29 PD patients and 12 healthy controls. Totally, eleven movement frequencies that ranges from 0.2 to 2.0 Hz with step size 0.2 Hz at four different amplitudes that ranges from 15 to 30 degrees with step size 5 degrees, were applied to the wrist. They concluded that rigidity scores were found at higher angular velocities are more reliable and has better correlation to the clinical rigidity scores given. Also, they found that mean rigidity score as 6.1 N.m-degree at rest and 7.2 N.m-degree at activated condition (with a contralateral hand maneuver) for normal.

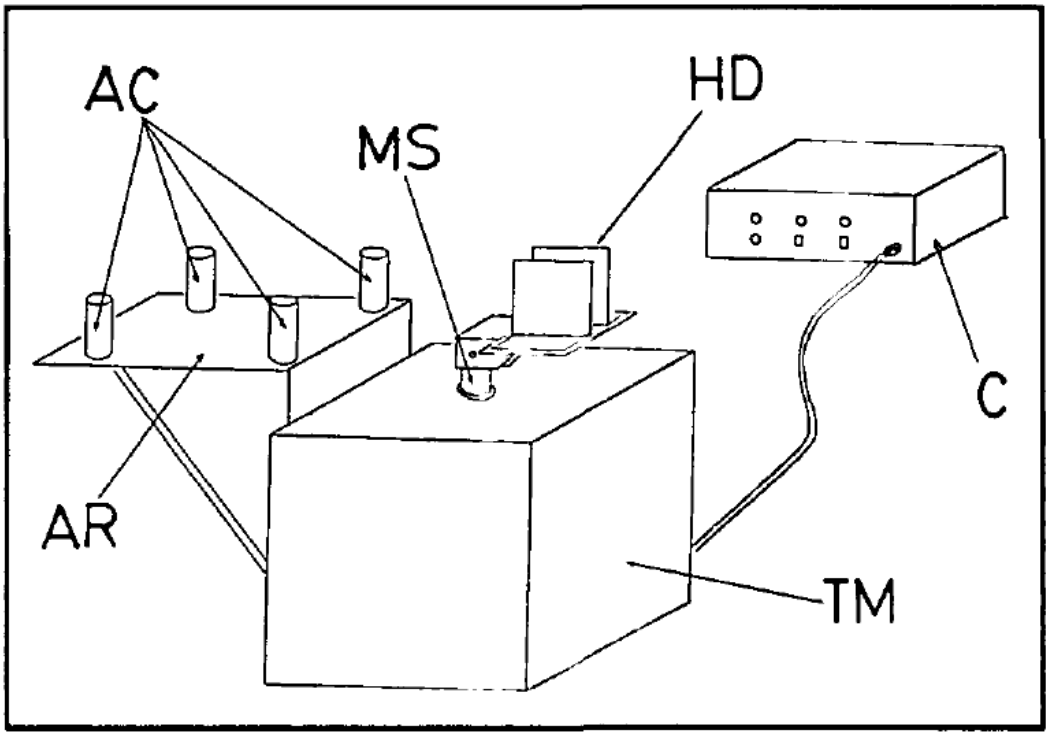


Figure 2.4. Schematic view of the apparatus used by Teräväinen *et al.* [13] AC : adjustable rubbers, AR: arm rest, MS: motor shaft, HD: handle, C: controller, TM: torque motor (reprinted from [13]).

Caligiuri [14] studied parkinsonian rigidity at the wrist with 29 patients and 25 healthy subjects. They used a portable transducer, shown in in Figure 2.5, with gyroscope and potentiometer to measure wrist rigidity. Clinical experiments were performed with and without a contralateral activation maneuver. The wrist was extended and flexed by the examiner within a 45° range of motion. They measured the applied force to the wrist and the corresponding angular displacement of the wrist. Instrumental rigidity scores of the participants were obtained by the computing the ratio of y-axis intercepts, which obtained by regressing the force data onto corresponding rotation data, for resting and active conditions. They performed experiments with 25 healthy controls, 18 non-rigid but at risk for developing rigidity and 11 PD. The PD participants presented the highest rigidity scores. In addition, they collected data from 4 PD patients in both "on" and "off" phases, the rigidity scores evaluated in the "off" phase were found higher than the scores in the "on" phase.

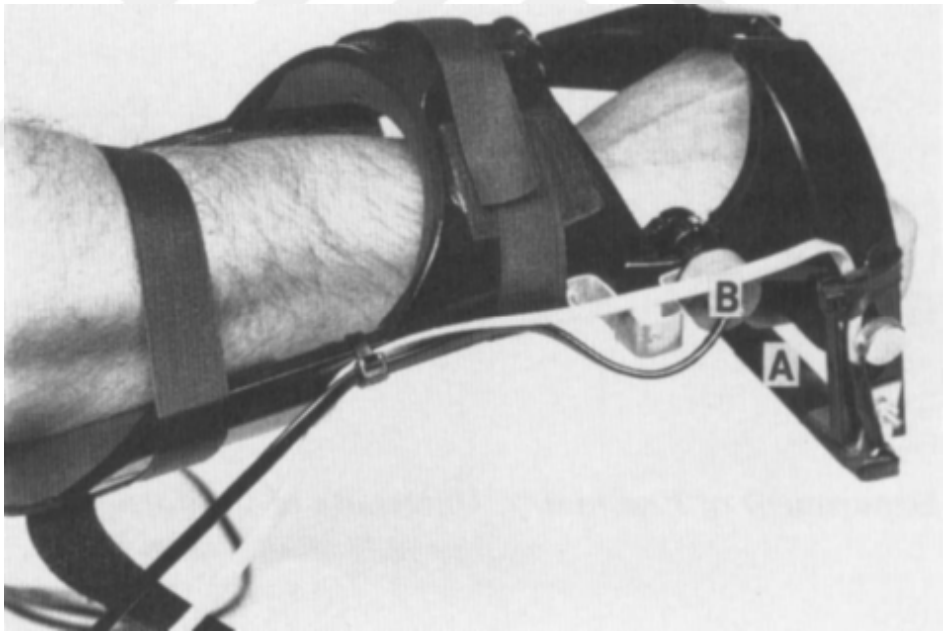


Figure 2.5. Transducer used by Caligiuri [14] to assess wrist rigidity. A: force gauge, B: rotation encoder (reprinted from [14]).

Fung *et al.* [15] published a study aiming to assess rigidity objectively by correlating total resistive force against to the passive movement of the wrist. They conducted experiments with 20 PD patients and 10 healthy controls.

They developed a manipulandum that supports and maintains the hand and it was mounted on the vertically orientated shaft driven by a torque motor. The torque generated by the motor was calculated from the current. In addition, to get angular position a potentiometer was used. The hand rotated through an arc of ± 45 ° degree both at 1 and 1.5 Hz with the torque motor. They integrated measured torque through the acquisition time, the result of this process is called "angular impulse score" by them. On the other hand, they also integrated the same torque data by angle and the result of this process called as the "work score". Both impulse and work scores of the patients were found higher than the control group. The results showed that the angular impulse scores showed higher correlation with clinical rigidity scores than the work scores.

Patrick *et al.* [16] published a study aiming the quantification of the UPDRS rigidity scale with a device having two air-filled pads connected to a differential force transducer to measure force applied to the pads. Device also contains a slide state piezo-electric gyroscope to measure the angular velocity. After mounting the device to the wrist, the examiner starts to extend and flex the wrist, repeatedly as shown in Figure 2.6.

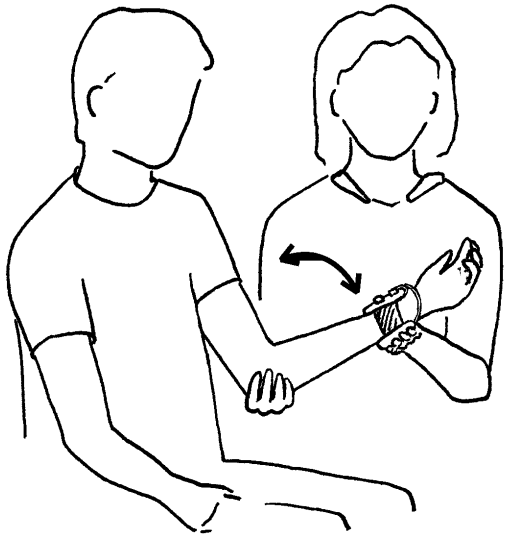


Figure 2.6. The use of the device to assess elbow and wrist rigidity designed by Patrick *et al.* [16]. The position of the device and forearm is different to assess wrist rigidity (not shown in the figure, reprinted from [16]).

The joint model not only includes elastic stiffness component but also viscous stiffness component as distinct from the previous studies in the literature. Mechanical impedance (Z) was calculated by taking magnitude of the vectoral sum of the modal parameters, then calculated impedance was used as the measurement of rigidity. While data acquisition process, the examiner also assessed the subject rigidity by her/his initiative. In addition, patients performed a contralateral activation maneuver for half of each trial. Without the activation maneuver, the mechanical impedance found to be 0.0114 $\pm$ 0.00498 N.m/degree for the wrist, with reinforcement Z values found as 0.0194 $\pm$ 00652 N.m/degree. In addition, they found Z values for control subjects as 0.00129 $\pm$ 0.00028 N.m/degree in non-reinforced condition. No effect on Z at the wrist in reinforcement condition. Their relationship between quantified mechanical impedance values and the UPDRS rigidity scores of the patients is presented in Figure 2.7.

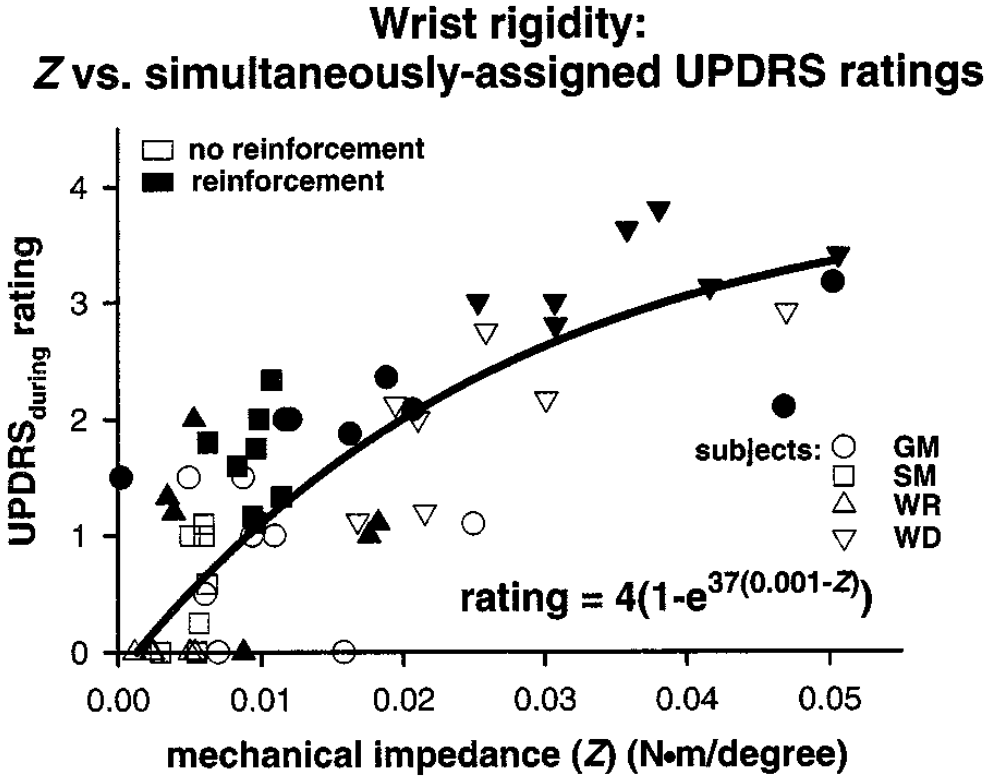


Figure 2.7. Relationship between measured mechanical impedance values and clinical rigidity scores of the subjects (reprinted from [16]).

Park *et al.* [17] researched viscoelastic properties of the wrist by a device shown in Figure 2.8. They adopted and tested three different mechanical wrist models. These models were identical in structure but different in the number of model parameters: first model has one damping and one spring constant, second model has two damping and one spring constant, and last model has two damping and two spring constants. They conducted experiments with 45 PD and 12 healthy subjects. Their major finding is that the first model which has one spring and one damping constant showed better correlation with clinical rigidity scores compared to other wrist models. They also showed that viscosity was more marked in subjects with greater clinical rigidity scores.

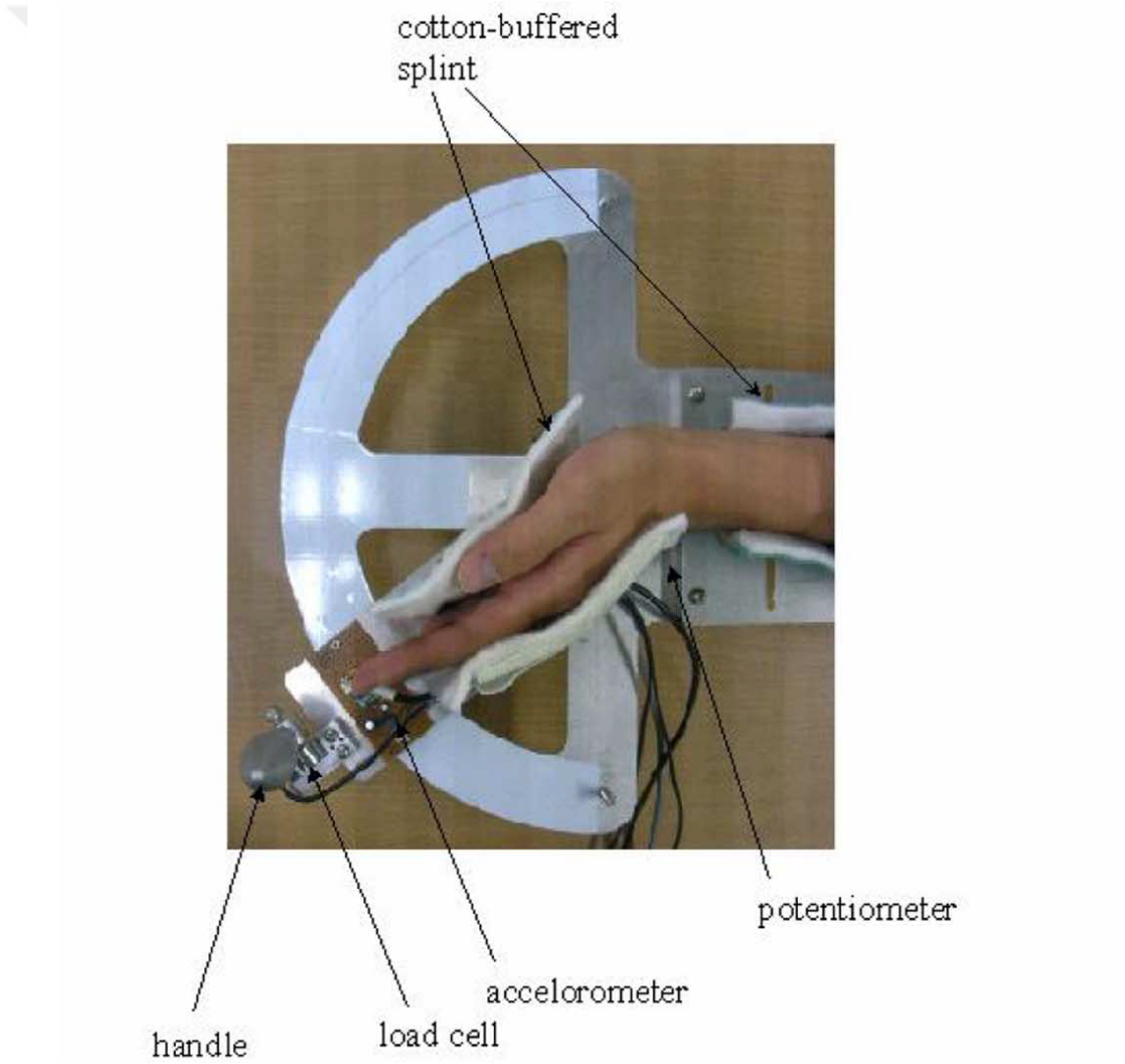


Figure 2.8. The use of the device designed by Park *et al.* [17] (reprinted from [17]).

Charles and Hogan [18] published a study which provided an experimentally based mathematical model of wrist rotation dynamics. They adopted a model consisting of inertial, damping, and stiffness terms. They found that the passive stiffness of the wrist is the major impedance to rotate wrist. On the other hand, inertial and damping terms only become important for relatively fast movements.

Endo *et al.* [19] analyzed parkinsonian rigidity at the elbow with a device composed of compact three-axis force sensors, a gyroscope, and surface electrodes. The rigidity measurements were performed with 27 PD patients and 24 healthy controls. Torque and angle were used to calculate elastic stiffness of the elbow. Although, they found a strong relationship between UPDRS rigidity score and elastic stiffness, no significant difference between the UPDRS 0 - 1, and UPDRS 3 - 4 groups was observed.

Considering the results of Charles [18] and Endo [19], the elastic stiffness can be used as a measurement of wrist rigidity. It can be calculated by using the Equation 2.1, where M is applied moment, θ is angular rotation, and K is stiffness constant. In this study, we adopted this equation to calculate wrist stiffness.

$$M = K\theta \tag{2.1}$$

3. MATERIALS AND METHODS

In this chapter, the proposed method to evaluate wrist rigidity via a smartphone in a clinical environment is presented.

3.1. Using Built-in Sensors of a Smartphone

Today's smartphones have various built-in environmental condition sensors such as accelerometer, gyroscope, magnetometer, light sensor, and pressure sensor providing raw data with high accuracy and precision. Sensor API gives the values of all registered sensors in the device coordinate system; however, these values can be written in a global coordinate system using sensor fusion techniques. The coordinate system of an android device are illustrated in Figure 3.1.

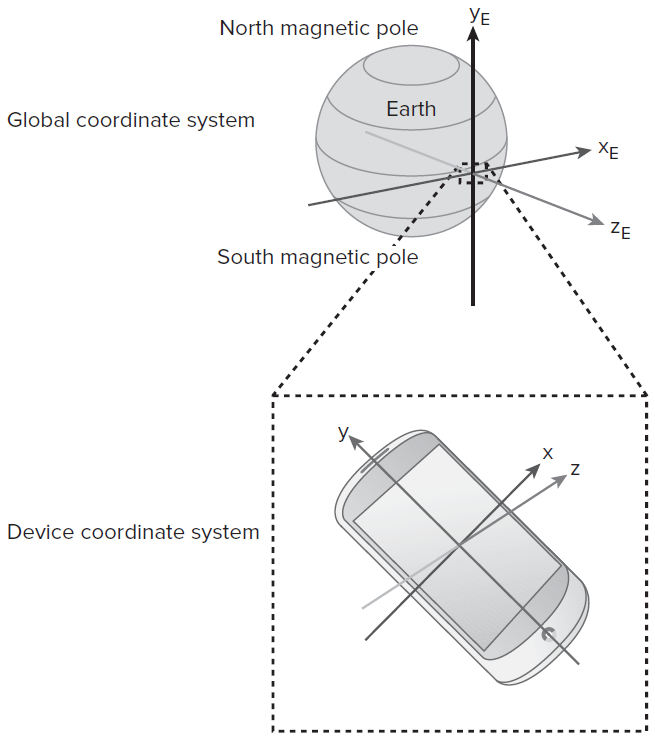


Figure 3.1. Global and device coordinate systems (reprinted from [20]).

In addition, other technologies like a capacitive touch screen, give additional information about user interactions with the device. In this study, all data were collected by a Samsung S10e which is powered by an Android 10 operating system[1] (OS). Dimensions and specifications of the phone are given in Appendix A. The selected device has no built-in force sensor to detect the applied force to the device screen. Although there is no force sensor in the device, the capacitive touch screen can be used to extract the force information from touch events on the device's screen. Android OS has various methods which can be used to obtain the details of a registered touch event on the screen such as its size and coordinates with respect to the device's screen.

3.1.1. Angle Detection

Built-in accelerometer sensors in smartphones have different technical specifications such as sampling rate and resolution. However, recent devices mostly have enough sampling rates reaching up to 512 Hz. The accelerometer values can be obtained using the Android sensor framework. Raw accelerometer data can be acquired by registering a sensor event listener, detailed explanation is presented in the Section 3.1.3.

The current orientation of a device can be obtained by merging data coming from three sensors: accelerometer, gyroscope, and magnetometer. A balance filter is adopted to merge sensor values. It integrates gyroscope data between successive sensor updates, and then high-pass filters the result to remove drift. Subsequently, this integrated and filtered gyroscope data are combined with accelerometer and magnetometer data which are low-pass filtered. The balance filter is described in Figure 3.2. The final summation to get device orientation is explained in Equation 3.1, where f is fused orientation, b is filter coefficient, g is gyroscope data, and d is orientation computed by accelerometer and magnetometer. The high filter coefficients further increase the effects of gyroscope data on the result; the filter coefficient b is picked as 0.98, this value was determined heuristically by testing different filter coefficients.

[1]The corresponding application program interface (API) level is 29.

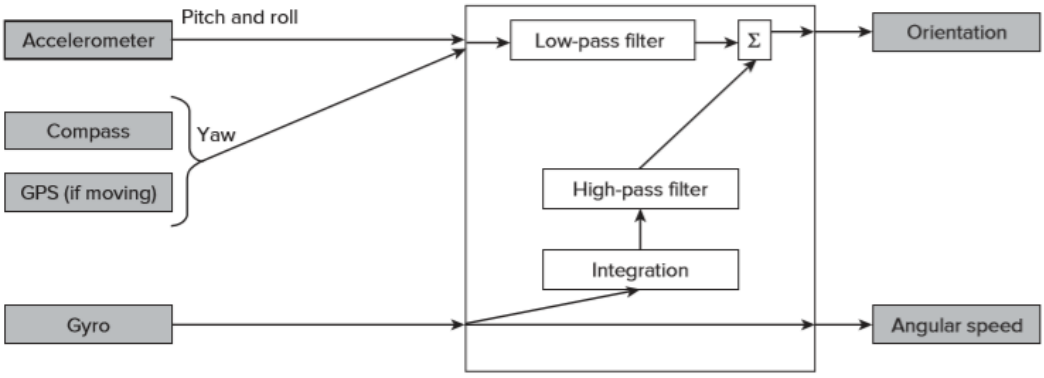


Figure 3.2. Schematic explanation of balance filter (reprinted from [20]).

$$f = b.g + (1 - b).d \tag{3.1}$$

3.1.2. Force Sensing Using Capacitive Touch Screen

In this subsection, the method for computing the force values applied to the device screen is presented. The force values cannot be directly obtained due to absence of an integrated force sensor; however, force can be derived from the area formed by the touch event on the device screen.

3.1.2.1. Information About Registered Touch Events. The Android *MotionEvent* class provides various methods to get information about touch events on the smartphone's screen. Our main aim is getting the area of the screen that is pressed. For this purpose, we used *getSize()* method that returns touch area that is normalized with the device screen size, touch size is scaled to a value between 0 and 1. The method gives new size values when touch size or the pointer on the screen is changed in terms of position or size; however, the sampling rate can be configured with a handler class that allows us to perform process at fixed time intervals.

3.1.2.2. Design and Manufacturing of a Touch Gadget. Capacitive touch screens are designed especially for the human finger; however, we decided to design and produce a new gadget that interacts with the phone screen in order to achieve a high inter- and intra-rater reliability. Capacitive touch screens sense the voltage drop on the screen when a pointer hits the screen. Therefore, the pointer must be conductive to achieve a successful touch event. Also, it must be deformable and soft enough not to damage the phone screen. A 3D model of the gadget and its molds are shown in Figure 3.3. The exact dimensions and detailed drawings of the components are given in Appendix A. The gadget consists of the parts 3 and 4 shown in Figure 3.3 (c). The parts 1 and 2 are not components of the gadget. They are just molds which are required for a silicone casting process. The material for the gadget's body were chosen as aluminum to make it electrically conductive. Thus, the body acts as a bridge between its deformable tip and the human body. The tip of the gadget was made of a mixture of rubber silicone and copper powder to achieve conductivity and compliance.

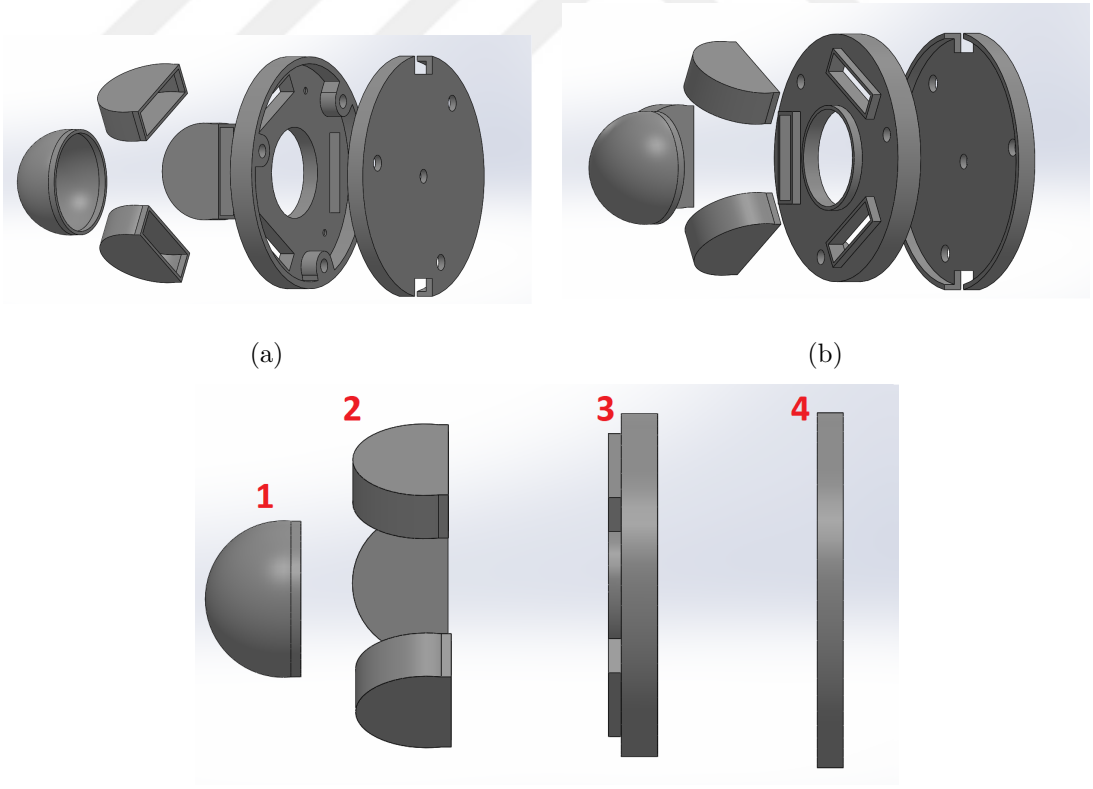
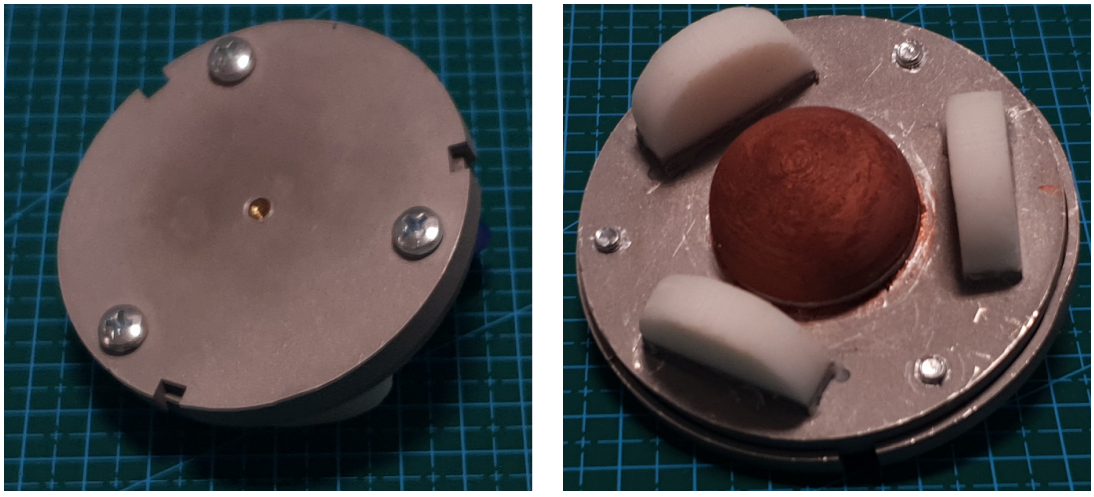


Figure 3.3. Exploded 3D model of the designed touch gadget: (a) and (b) isometric views, (c) side view.

A mixture of copper powder and rubber silicone poured into the mold indicated with the label 1 in Figure 3.3 (c). The mixture consists of %75 silicone rubber and %25 copper powder by weight. The mixture was cured at room temperature for 24 hours. The technical information of the used silicone rubber and copper powder are given in Appendix A. On the other hand, silicone rubber which does not contain any conductive filler was poured into the molds indicated with the label 2 in the same figure. The hardness difference of these different type of silicone rubbers is not experimentally measured; however, the silicone rubber at the center of the gadget may have higher hardness value than the support rubbers. The conductive filler increases the hardness of silicone rubber. The molds have the same height. After the curing process, molds are removed. The manufactured touch gadget is shown in Figure 3.4.

Alternatively, different gadget designs can be adopted for the same purpose. For instance, all contact parts of the gadget can be conductive, or the shape of the contact components can be different in another design. The design which has only one conductive contact pointer was adopted in order to make the computation of the touch area easier.



(a) (b)

Figure 3.4. The manufactured touch gadget to convert capacitive touch sensor output to force: (a): back of the gadget where the force is applied, (b): front of the gadget touching the phone screen.

3.1.2.3. Calibration of the Gadget. We conducted a calibration process to reveal the relationship between the area stem from a touch event and the corresponding force. An experimental setup has been developed for this purpose. An illustration of the setup is shown in Figure 3.5. An ATI Nano 17 force/torque sensor was used, and the output of the sensor was converted to force measurements using the LabView software. The force sensor was fixed to the back of the phone, then the gadget was aligned to the center of the phone screen. A parallel beam mechanism was used to prevent lateral forces during the calibration. Hence, the gadget is constrained to move vertically. Forces were applied in the direction of the red arrow shown in Figure 3.5 by the operator's thumb. The gadget was periodically pressed and released for 41 times without any interruption.

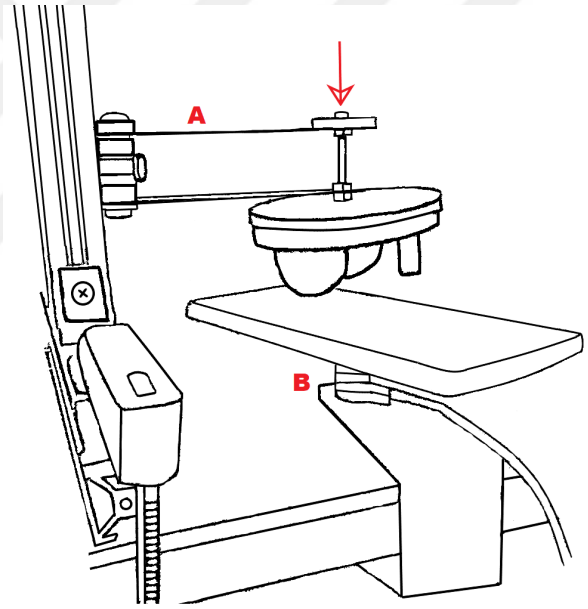
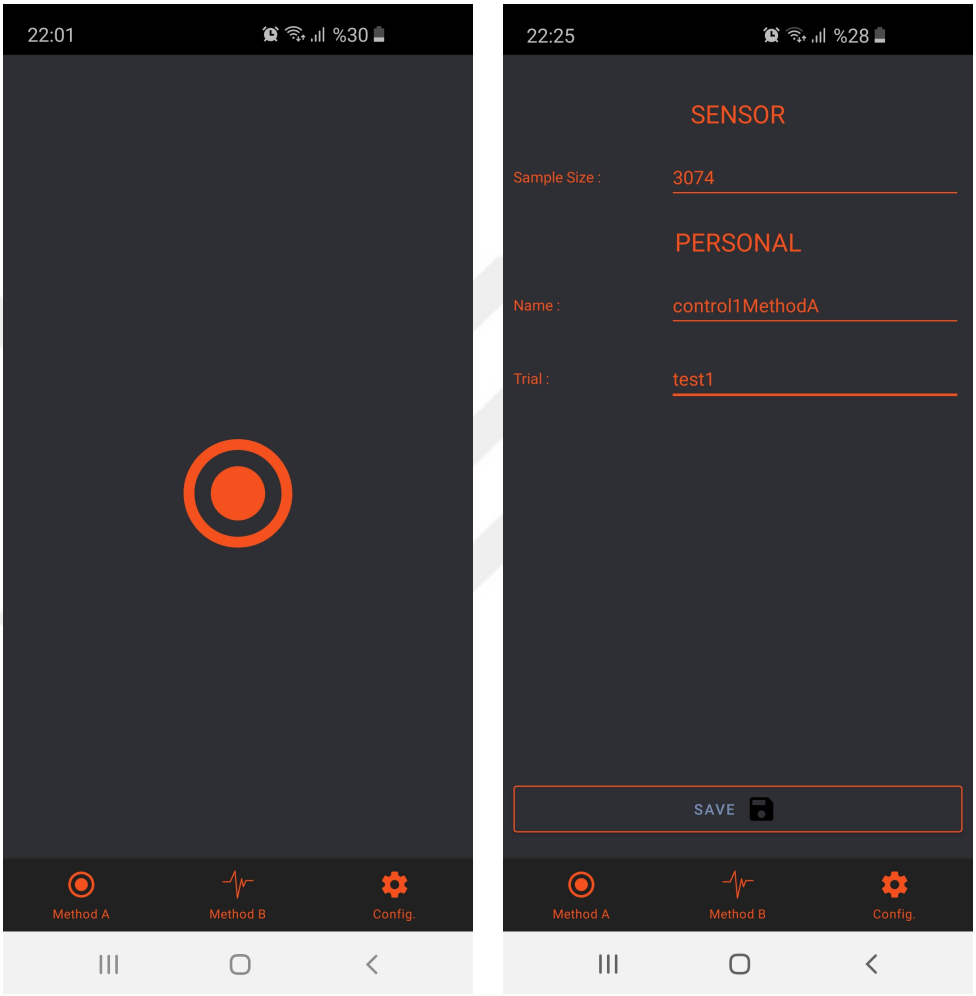


Figure 3.5. The schematic presentation of the calibration process. A: parallel beam mechanism, B: force sensor.

3.1.3. Developed Smartphone Application

In order to collect sensor data during the calibration process and the clinical experiments, an Android application has been developed. The application has three screens; however, in this study only two pages as shown in Figure 3.6 are used.

The other screen named as “Method B” is designed for a parallel study which assess wrist rigidity with a different approach by Züngör [21]. The screen shown in Figure 3.6 (a) is the main screen of the application. The second screen is the configuration screen designed to change the sample size, and gather the information about the trials.

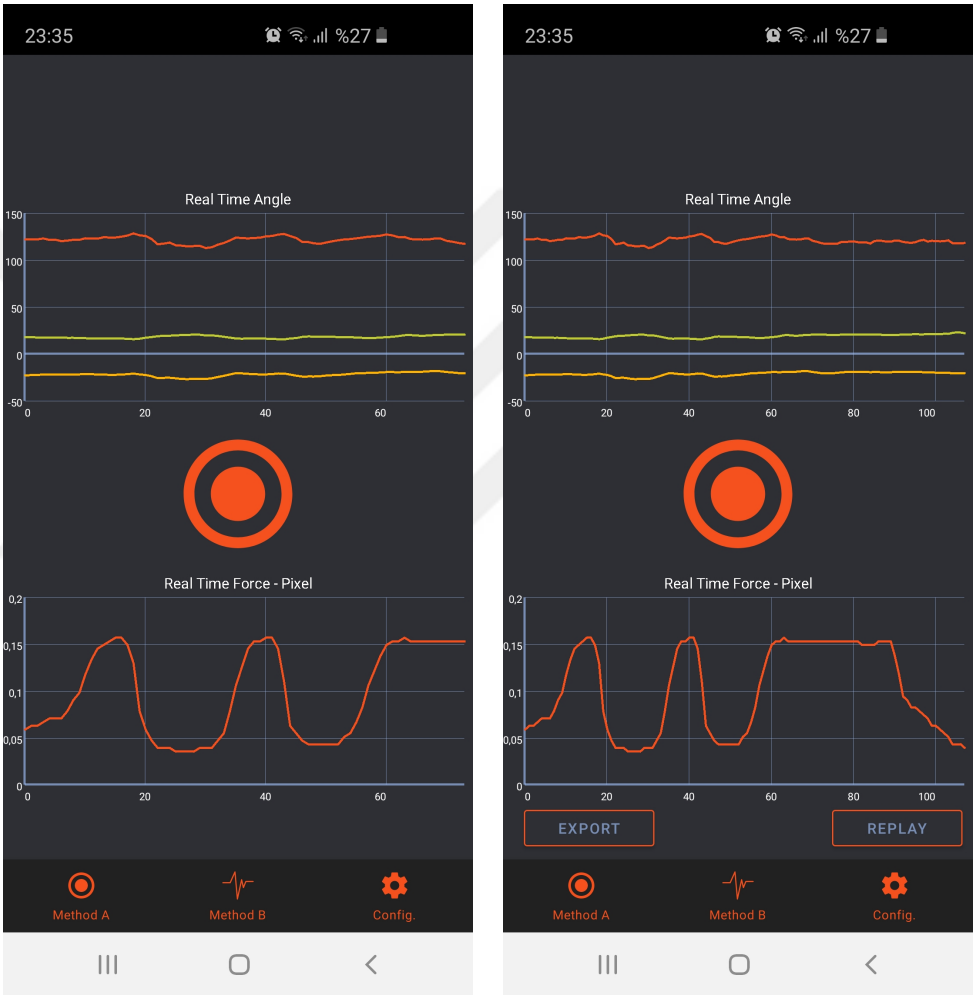


(a) (b)

Figure 3.6. Screenshots of the designed application: (a) main screen, (b) configuration screen.

If a pointer hits the image indicated on the main screen of the application, the application senses the first touch, and then starts to collect sensor output until the pointer leaves the surface of the screen. If the pointer leaves the screen, the application stops to read new sensor values, and asks the user to export the data as shown in Figure 3.7 (b).

The Unified Modelling Language (UML) class diagram of the application is shown in Figure 3.8. *SensorObservable* class listens new sensor outputs with the method *onSensorChanged()*, and then notifies the registered listener *SensorObserver*. *SensorObserver* stores the new sensor outputs in lists, if desired data size reached listener unregisters the *SensorObservable*. Lists have three rows for sensor outputs in x, y and z axes.



(a) (b)

Figure 3.7. After the first touch occurred on the screen, the application starts to collect touch area and orientation of the device: (a) shortly after the touch event registers, (b) the touch event is over.



Figure 3.8. UML class diagram of sensor-related clasesses of the application.

3.1.4. Remote File Transfer Server for Data Storage

The application does not necessarily need a remote file transfer (FTP) server to store sensor data; however, storing data remotely is more secure than keeping files in the smartphone memory. Moreover, remote storage enables to form a database. We used a standard compute engine which is a virtual machine (VM) hosted on Google Cloud Platform (GCP). The engine has one virtual central processing unit (vCPU), 3.75 gigabyte (GB) memory, 50 GB storage capacity, and a CentOS 7 operating system. The FTP server was written with the Golang programming language which also known as Go.

3.2. Experimental Methods

Clinical experiments were conducted to prove that the gadget and the phone application can be used to evaluate wrist rigidity in PD patients. 11 healthy controls and 10 PD patients voluntarily participated in the experiments. The experimental protocol is approved by Institutional Review Board of Ankara University School of Medicine. There was at least one neurologist from the Department of Neurology of Ankara University School of Medicine in charge during the experiments.

3.2.1. Procedure

The procedure was designed for the right hand of each participant. Prior to the trials, the following steps were performed:

- As shown in Figure 3.9, a black thin cushion (F) was fixed on a table by a glue prior to the experiments. It was located at the corner of the table such that the subject could put his/her forearm comfortably on it while sitting a chair (E) near the table. Medical elastic straps (A and B) in Figure 3.9, were stitched to this fabric. The forearm of the subject was fixed on the table with these straps.
- The informed consent form was read to the participant, then the form was signed by the participant. In addition, the neurologist in charge signed the same form.

- Patient follow-up and UPDRS forms were fully filled by the neurologist and stored in a way that is pursuant to the ethical guidelines.
- The subjects were encouraged to remain calm throughout the clinical trials. They were informed about the content of the trials. It was explained that the participants should not resist to wrist movements which is performed by the operator.

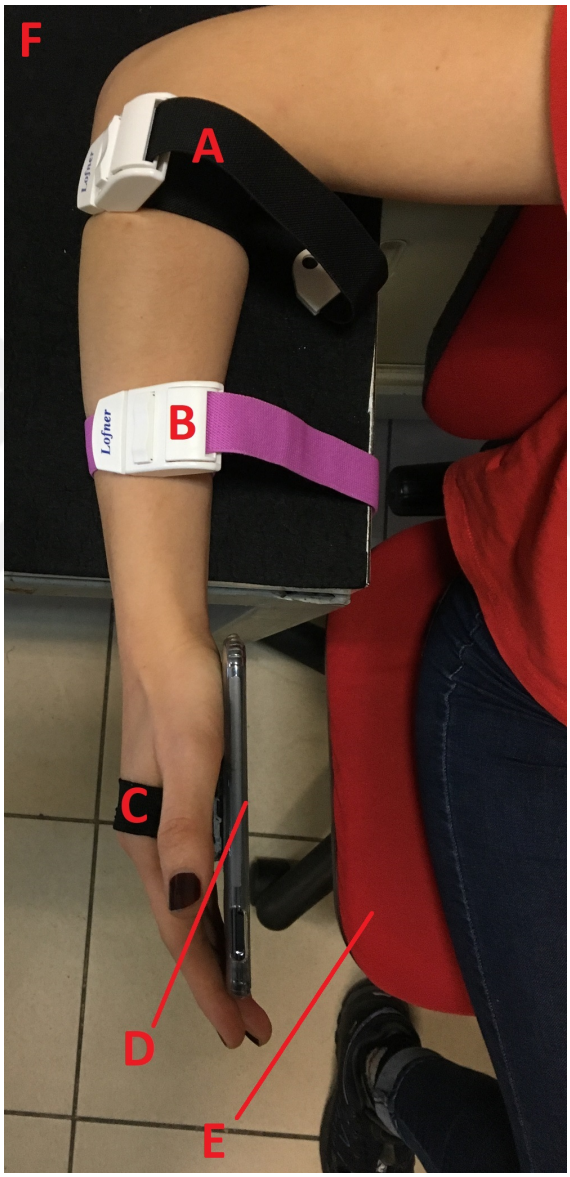
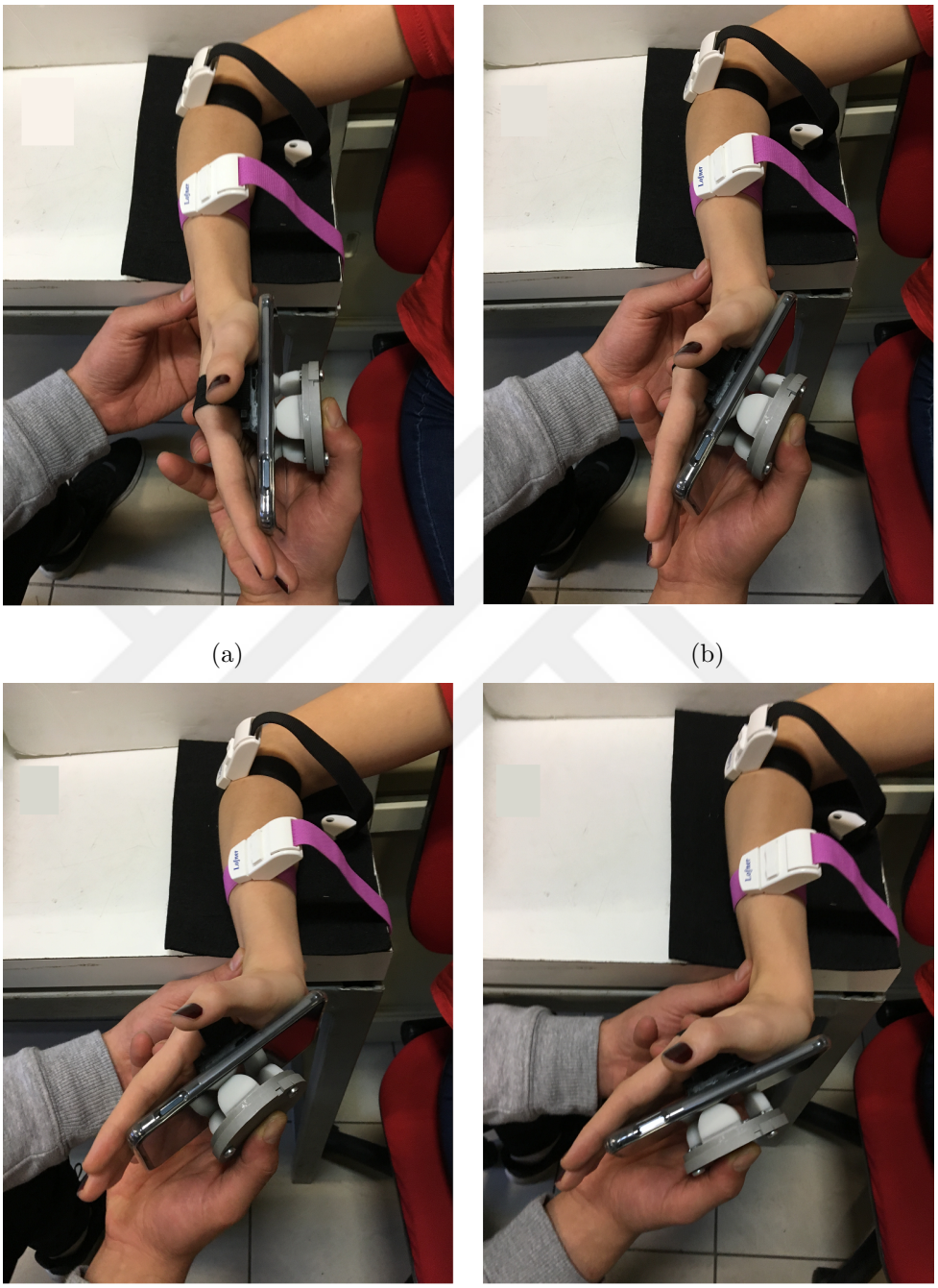


Figure 3.9. The forearm posture during the experimental trials: A and B are medical loop straps to fix the forearm to a table, C is an apparatus to fix the smartphone to the hand, D is a case for the phone, E is a chair for subjects to sit, and F is a thin cushion to make the forearm comfortable.

A copy of the patient follow-up and the informed consent forms are given in Appendix B. After the above steps were completed, the following steps were performed:

- The input fields on the configuration screen of the application were filled by the operator performing the experiment, then the smartphone was placed to the phone case.
- The gadget was centered on the screen of the phone. The wrist of the subject was held with the left hand of the operator performing the experiment as in Figure 3.10 (a). A slight force was applied to the gadget with the right thumb of the operator, while the other fingers of the right hand were positioned to support the hand of the subject.
- When the phone started to collect data, the applied force was gradually increased, and the hand was rotated around the wrist until the angle reaches of rotation 50-70°. This motion was tried to be performed only with the force applied by the thumb. The hand was moved by rotating it from the initial position to the final position which are shown in Figures 3.10 (a) and (d). After reaching the final position, the applied force was released and hand was rotated back to the initial position. This cyclic motion was repeated 10 times.
- The gadget was removed from the screen after 10 repetitions. The phone was removed from the case and the data collected during the experiment was examined. If any abnormality such as a touch failure or a gadget displacement on the phone screen during the experiment was observed, the experiment was repeated, otherwise data was sent to the remote server.
- The described steps above were repeated 10 times for each subject.

The whole experiment was also performed with a contralateral activation maneuver after a 5-minute break for the subject to rest. In addition, the subjects with PD were participated to the experiments both in "on" and "off" conditions. On condition refers the improvement of symptoms by anti-parkinsonian medications or DBS, off condition refers the aggravation of symptoms due to withdrawal of medications or turning off DBS. Likewise, a 5-minute break was given between these experiments.



(a) (b)

(c) (d)

Figure 3.10. Rotation of the hand about the wrist by the force applied to the gadget with the right thumb of the operator: (a) the initial position of the loading cycle, (b) and (c) intermediate positions, (d) the final position of the loading cycle.

3.2.1.1. Froment Maneuvers Performed in the Trials. In consultation with the neurologists, two diffrent Froment maneuvers (voluntary contralateral activities) were selected to be performed in the experiments. For the first activity, the patients were asked to fully outstretch their opposite arm, and then asked to touch their nose with the tip of their index finger, after that the patient was asked outstretch their arm again. This finger-to-nose movement is shown in Figure 3.11. For the second activity, the subjects were first asked to raise their hand, and then open and close it periodically as shown in Figure 3.12.



(a) (b)

Figure 3.11. The first contralateral activity: (a) the index finger is away from the face, (b) the index finger touches the patient's nose. The subjects were asked to perform this activity periodically.



(a)



(b)

Figure 3.12. The second contralateral activity: (a) the hand is closed, (b) the hand is opened. The subjects were asked to perform this activity periodically.

3.2.1.2. Randomization of Experimental Trials. The clinical trials to assess wrist rigidity were performed with each subject in two condition: with and without a contralateral activation maneuver. In addition, participants with PD were asked to perform additional trials both in “on” and “off” periods. The order of these trials was randomized to alleviate the selection bias and to insure against the accidental bias. The randomized orders of experiments are presented in Table 3.1. The second column indicates the order of conditions “on” and “off”. For instance, “Off - On” in the first row indicates that the experimental trials in ”off” condition was performed prior to “on” condition. Similarly, the third column shows the order of trials where the activation maneuver was performed or not. “0 ” indicates the trials where no activation maneuver performed, and “F” indicates the trails where rigidity measured with an activation maneuver. The last column of the table indicates which maneuver was adopted: “1” stands for the first maneuver discussed in the previous section, and “2” stands for the second maneuver.

Table 3.1. The table of randomized trials for PD patients and controls.

Participant	**On-Off Order**	**Activity Order**	**Maneuver Type**
Subject 1	Off - On	0 - F	2
Subject 2	Off - On	0 - F	2
Subject 3	Off - On	F - 0	1
Subject 4	On - Off	F - 0	1
Subject 5	Off - On	0 - F	2
Subject 6	Off - On	F - 0	1
Subject 7	Off - On	F - 0	1
Subject 8	On - Off	0 - F	1
Subject 9	On - Off	F - 0	2
Subject 10	On - Off	F - 0	1
Control 1	-	0 - F	1
Control 2	-	0 - F	2
Control 3	-	F - 0	2
Control 4	-	0 - F	2
Control 5	-	F - 0	1
Control 6	-	F - 0	1
Control 7	-	0 - F	2

Table 3.1. The table of randomized trials for PD patients and controls. (cont.)

Participant	On-Off Order	Activity Order	Maneuver Type
Control 8	-	0 - F	2
Control 9	-	F - 0	1
Control 10	-	0 - F	1
Control 11	-	F - 0	2

3.2.2. Subjects

Totally, 10 subjects with PD and 11 healthy controls were participated in the clinical experiments. The UPDRS rigidity scores of each participant assessed by the neurologist accompanying the experiments are given in Table 3.2. The term UPDRS rigidity score will be called as clinical rigidity score (CRS) in next chapters.

Table 3.2. CRSs of the PD patients and healthy controls.

Participant	CRS	Participant	CRS in Off Condition	CRS in On Condition
Control 1	1	**PD 1**	2	1
Control 2	1	**PD 2**	3	4
Control 3	0	**PD 3**	1	0
Control 4	0	**PD 4**	3	1
Control 5	0	**PD 5**	2	1
Control 6	1	**PD 6**	2	1
Control 7	0	**PD 7**	2	1
Control 8	1	**PD 8**	4	3
Control 9	1	**PD 9**	2	1
Control 10	1	**PD10**	0	0
Control 11	1			

3.2.3. Calculation of Elastic Stiffness

Force and angle data are used to calculate elastic stiffness of the wrist. The force is multiplied by the moment arm to calculate the applied moment to the wrist, then

the moment is divided by the angle. Subsequently, a linear line is fitted to this data. For instance, exported force and angle data for subject 8 is given Figure 3.13. The lines between each red and yellow dots indicate the extension movements of the wrist. Fitted stiffness lines are presented in Figure 3.14.

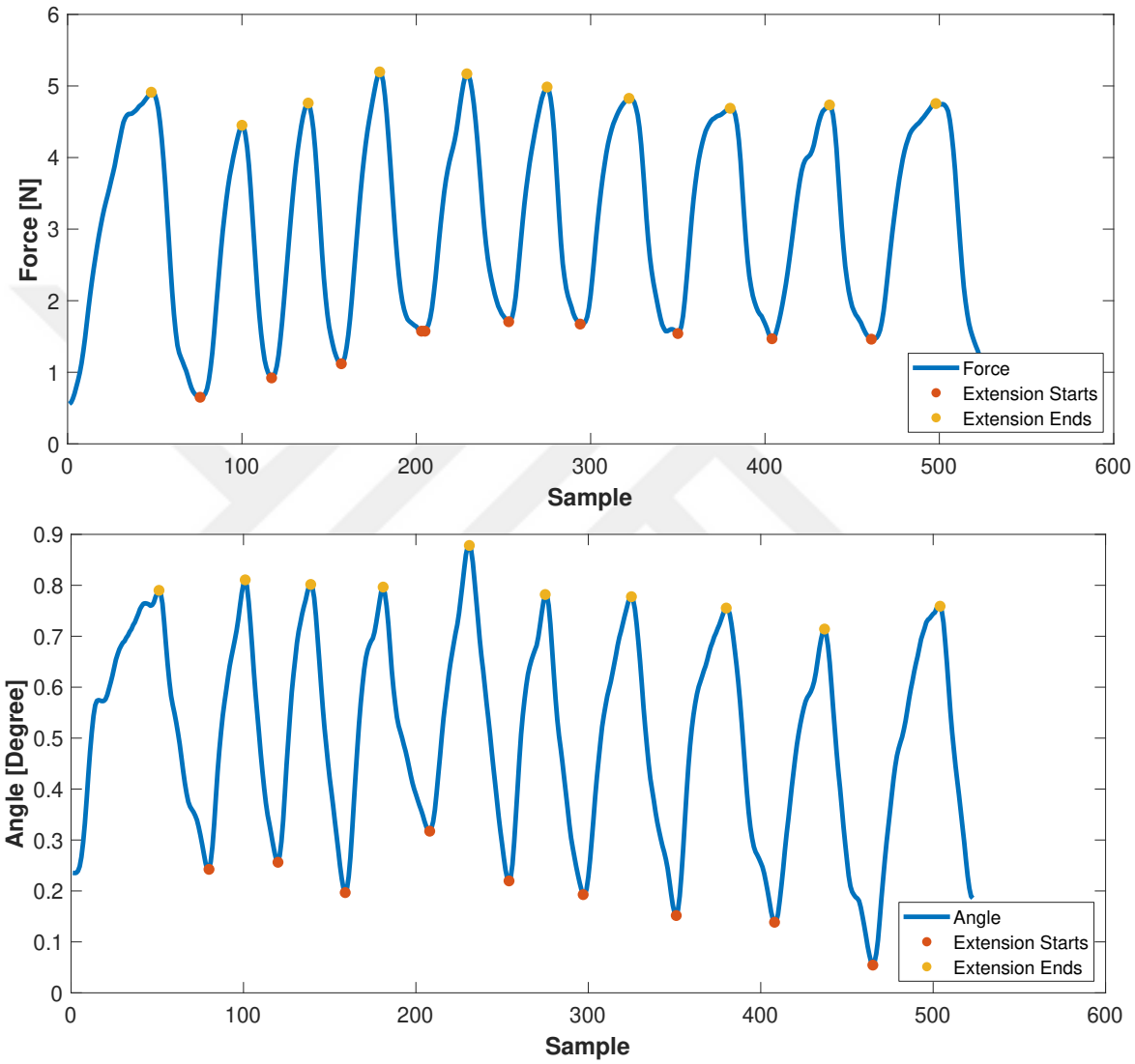


Figure 3.13. Exported angle and force data of PD patient 8.

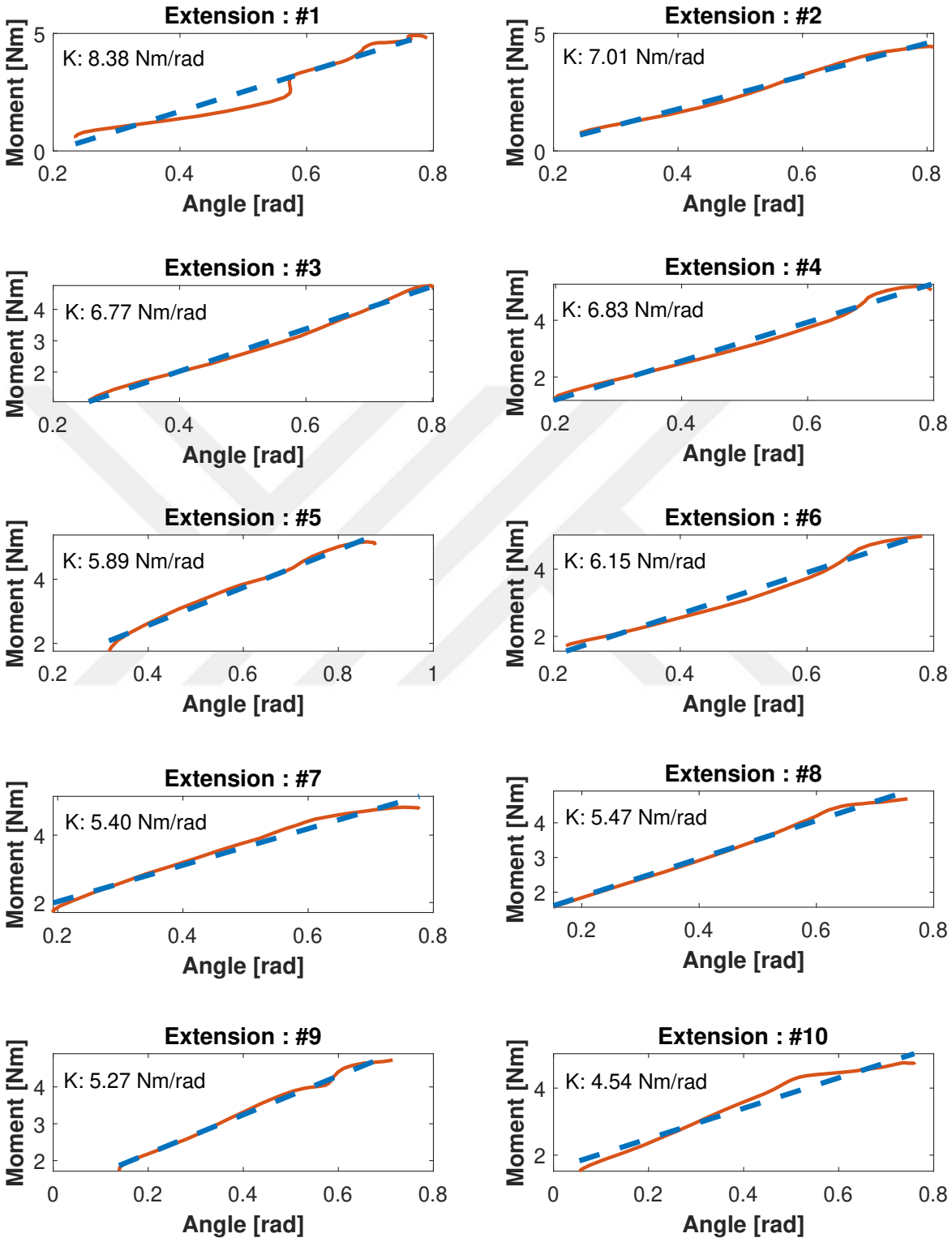


Figure 3.14. Stiffness lines fitted to moment-angle data.

4. RESULTS AND DISCUSSION

In this chapter the results of the calibration of the gadget and conducted trials with subjects are presented.

4.1. Calibration Results

The calibration cycles are plotted in Figure 4.1. To find the relationship between touch area and force, linear regression analysis was performed.

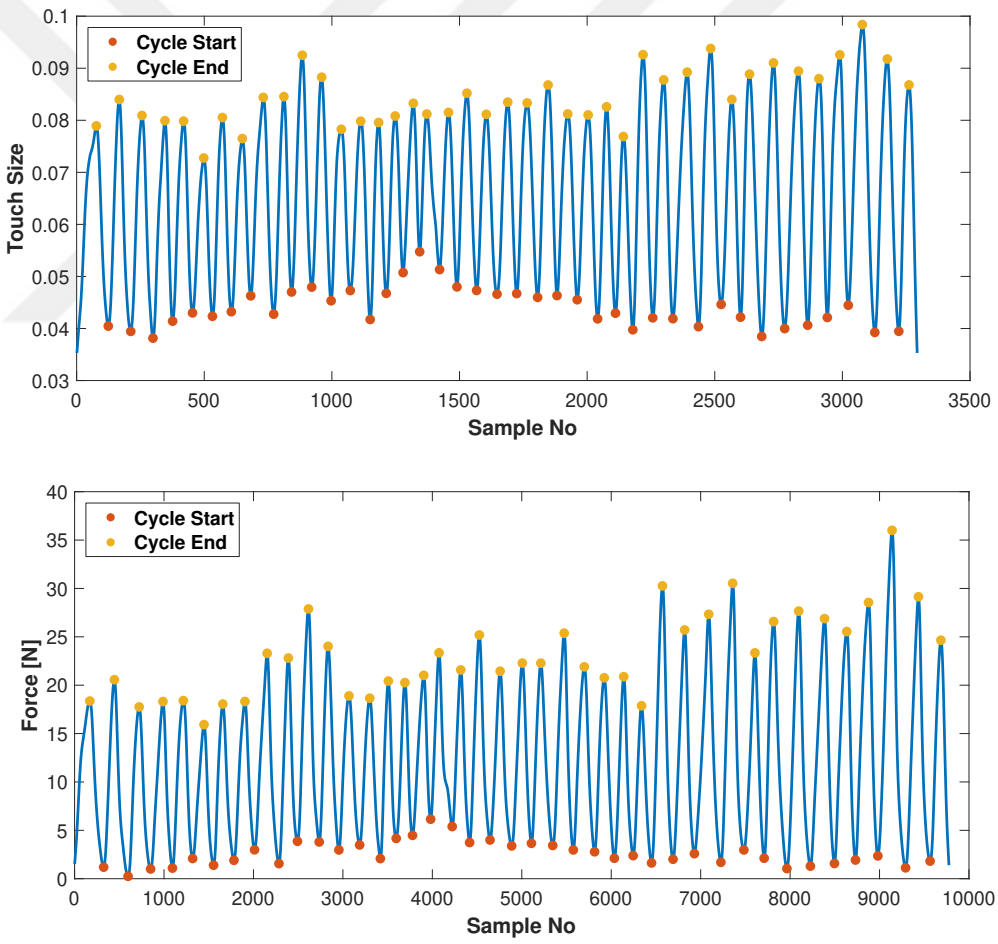


Figure 4.1. Data collected from the capacitive touch screen and the force sensor during the calibration process: normalized touch sizes acquired from the smartphone (top), and measured forces (bottom).

Obtained lines for each loading cycle are presented Table 4.1. We can compute mean regression line by averaging coefficient of linear lines found for every cycle due to linearity of regression lines. The slope was found as 489.05 and the intercept term was found as 19.36. The independent variable of the calibration function is touch area. Measured force against measured touch sizes are plotted in Figure 4.2. The mean calibration line is also shown in this figure. High pixel areas are not linearly convertible to the force as can be seen from the figure.

Table 4.1. Linear regression results of each calibration cycle.

Cycle No.	**Regression Line**	**R^2**	**Cycle No.**	**Regression Line**	**R^2**
#1	$363.88x - 10.41$	0.9869	**#22**	$486.37x - 19.24$	0.9942
#2	$438.35x - 16.31$	0.9996	**#23**	$489.97x - 19.82$	0.9876
#3	$426.88x - 16.51$	0.9992	**#24**	$517.73x - 21.14$	0.9913
#4	$413.68x - 15.44$	0.9894	**#25**	$533.77x - 22.04$	0.9978
#5	$453.56x - 17.59$	0.9997	**#26**	$499.96x - 20.12$	0.9991
#6	$445.85x - 17.33$	0.9912	**#27**	$449.55x - 16.80$	0.9983
#7	$424.516x - 16.32$	0.9988	**#28**	$447.32x - 16.88$	0.9988
#8	$479.78x - 18.66$	0.9992	**#29**	$529.11x - 20.70$	0.9848
#9	$517.60x - 21.95$	0.9807	**#30**	$480.91x - 18.91$	0.9770
#10	$498.67x - 19.85$	0.9985	**#31**	$486.30x - 19.25$	0.9634
#11	$520.86x - 20.63$	0.9994	**#32**	$519.01x - 20.25$	0.9883
#12	$488.15x - 19.44$	0.9993	**#33**	$488.10x - 19.45$	0.9837
#13	$469.25x - 18.92$	0.9856	**#34**	$515.59x - 19.87$	0.9990
#14	$456.17x - 17.59$	0.9966	**#35**	$490.24x - 18.66$	0.9892
#15	$469.96x - 17.48$	0.9988	**#36**	$483.64x - 18.42$	0.9875
#16	$454.59x - 17.70$	0.9839	**#37**	$486.07x - 17.80$	0.9973
#17	$507.63x - 21.43$	0.9999	**#38**	$517.45x - 21.10$	0.9833
#18	$619.64x - 28.31$	0.9869	**#39**	$614.27x - 26.96$	0.9806
#19	$529.99x - 22.29$	0.9959	**#40**	$504.28x - 19.73$	0.9834
#20	$563.47x - 24.07$	0.9897	**#41**	$473.72x - 18.28$	0.9830
#21	$495.44x - 20.10$	0.9821			
Mean	**489.05x-19.36**				

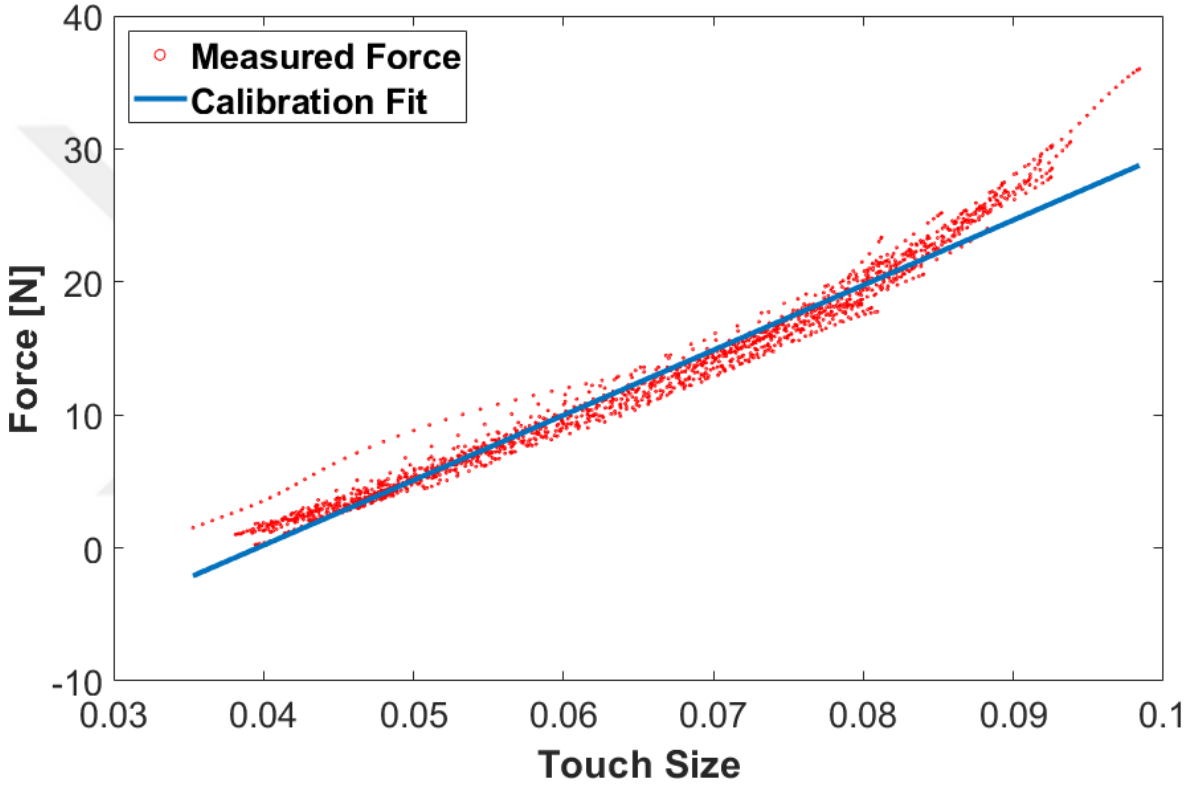


Figure 4.2. Measured force vs touch sizes. The calibration line is shown with blue solid line.

4.2. Rigidity Measurement Results

Each PD patient has four data sets coming from "on-off" and "resting-activated" conditions. The descriptive statistics about these data sets are presented in Table 4.2. The abbreviations OFF+NF and ON+NF in the table indicate the clinical trials without a contralateral activation maneuver (NF stands for no Froment maneuver), for off and on periods, respectively. Conversely, OFF+F and ON+F indicate the clinical trials where the participants performed a contralateral activation maneuver (F stands for a Froment maneuver), for off and on periods, respectively. Q1, Q3 and N in the table header stand for first quartiles, third quartiles and total data size, respectively. Total data size does not indicate the total trial size but total torque-angle cycle size. There are approximately 10 to 20 torque-angle cycles in a single trial, and at least 5 trials were performed for a single subject. Standard error of the mean (SE Mean), standard deviations (StDev), medians (Med), maximum (Max) and minimum (Min) stiffness values are also given in the table.

The highest mean stiffness was 11.21 N.m/rad which was for subject 8. This computed stiffness value confirms the CRS of the subject 8. Similarly, the lowest stiffness values were 0.64 and 0.66 N.m/rad for subjects 3 and 10, respectively. These computed stiffness values confirm the low CRS for both subjects. The data sets of subject 2 were excluded from further analyses due to hardware problems. Although the highest and lowest stiffness values seem to match given CRSs, further statistical tests were performed to prove that the computed stiffness values can be correlated with the CRS.

The stiffness values were grouped by the corresponding CRSs. The group statistics are given in Table 4.3. The individual stiffness values of the CRS groups are plotted in Figure 4.3 including both "on" and "off" conditions. We applied the Anderson-Darling test to each group to determine whether the data follow a normal distribution or not ($\alpha = 0.05$). The test results are given in the last column of the table. The p-values greater than the significance level of 0.05. Therefore, we have enough evidence to conclude that individual stiffness values of the CRS groups are normally distributed.

Table 4.2. Descriptive statistics about the data collected from PD patients.

S. No.	Trial	N	CRS	Mean	SE Mean	StDev	Min	Q1.	Med.	Q3	Max
1	OFF+NF	61	2	1.55	0.07	0.56	0.54	1.20	1.48	1.91	2.74
	ON+NF	67	1	1.11	0.04	0.31	0.33	0.89	1.05	1.37	1.89
	OFF+F	41	*	1.59	0.11	0.68	0.33	1.10	1.53	2.10	3.16
	ON+F	75	*	1.10	0.04	0.38	0.46	0.82	1.03	1.36	2.20
3	OFF+NF	68	1	1,36	0,05	0,38	0,64	1,08	1,32	1,62	2,16
	ON+NF	88	0	0,64	0,02	0,16	0,36	0,54	0,61	0,71	1,39
	OFF+F	89	*	1,38	0,03	0,32	0,54	1,15	1,39	1,62	2,04
	ON+F	101	*	0,83	0,02	0,19	0,12	0,71	0,84	0,96	1,33
4	OFF+NF	80	3	2,82	0,07	0,61	1,5	2,42	2,77	3,1	4,85
	ON+NF	59	1	1,31	0,12	0,88	0,2	0,81	1,11	1,5	5,98
	OFF+F	82	*	3,67	0,11	0,98	1,9	2,96	3,52	4,4	6,75
	ON+F	78	*	1,25	0,09	0,84	0,0	0,76	1,18	1,6	5,18
5	OFF+NF	69	2	1,59	0,10	0,85	0,23	1,18	1,44	1,79	6,12
	ON+NF	91	1	0,92	0,03	0,26	0,39	0,76	0,89	1,08	1,86
	OFF+F	55	*	1,59	0,14	1,03	0,08	1,01	1,34	2,06	5,09
	ON+F	80	*	0,94	0,02	0,19	0,59	0,77	0,92	1,06	1,43
6	OFF+NF	51	2	1,32	0,03	0,20	0,84	1,17	1,32	1,47	1,74
	ON+NF	59	1	1,24	0,03	0,25	0,53	1,12	1,23	1,41	1,90
	OFF+F	52	*	1,54	0,03	0,25	0,61	1,41	1,54	1,72	2,12
	ON+F	62	*	1,55	0,04	0,28	1,08	1,35	1,52	1,77	2,41
7	OFF+NF	58	2	1,14	0,03	0,24	0,71	0,97	1,13	1,26	1,95
	ON+NF	66	1	1,17	0,03	0,27	0,58	1,01	1,11	1,30	2,06
	OFF+F	57	*	1,36	0,04	0,26	0,84	1,21	1,38	1,49	2,08
	ON+F	53	*	1,54	0,05	0,37	0,74	1,31	1,49	1,69	2,83
8	OFF+NF	63	4	4,61	0,36	2,83	1,18	3,27	3,89	5,20	16,25
	ON+NF	51	3	2,26	0,16	1,11	1,07	1,66	2,01	2,43	8,27
	OFF+F	51	*	11,21	1,12	7,99	2,23	5,71	7,90	14,82	42,22
	ON+F	48	*	6,01	0,27	1,87	3,01	4,54	5,98	7,20	10,90
9	OFF+NF	72	2	1,75	0,11	0,90	0,28	1,26	1,58	2,12	6,41
	ON+NF	47	1	1,40	0,10	0,69	0,05	1,06	1,33	1,93	2,98
	OFF+F	64	*	3,12	0,27	2,12	0,30	1,73	2,67	4,03	11,91
	ON+F	48	*	1,57	0,11	0,76	0,48	1,01	1,52	1,89	4,41
10	OFF+NF	61	0	0,66	0,01	0,09	0,45	0,59	0,68	0,72	0,84
	ON+NF	60	0	0,70	0,02	0,12	0,46	0,61	0,69	0,77	0,98
	OFF+F	60	*	0,73	0,02	0,15	0,43	0,60	0,74	0,83	0,97
	ON+F	61	*	1,20	0,06	0,49	0,05	0,85	1,24	1,50	2,46

* In clinical practice, this maneuver is only used for differentiating CRS-0 from CRS-1.

Applying a normality test to these data sets may be futile; however, we did not want to violate the assumptions of further statistic tests, especially for one-way ANOVA analysis. The group CRS-4 was excluded from the further tests because the group has no standard deviation.

Table 4.3. Descriptive statistics about the clinical rigidity groups.

Group	**N**	**Mean**	**S.E. Mean**	**St.Dev.**	**Min.**	**Q1.**	**Med.**	**Q3**	**Max.**	**p-value**
CRS-0	3	0,67	0,02	0,03	0,64	0,64	0,66	0,70	0,70	0.487
CRS-1	7	1,22	0,06	0,17	0,92	1,11	1,24	1,36	1,40	0.717
CRS-2	5	1,47	0,11	0,24	1,14	1,23	1,55	1,67	1,75	0.692
CRS-3	2	2,54	0,28	0,40	2,26	*	2,54	*	2,82	0.227
CRS-4	1	4,61	*	*	4,61	*	4,61	*	4,61	*

*Could not be calculated because of the small data size.

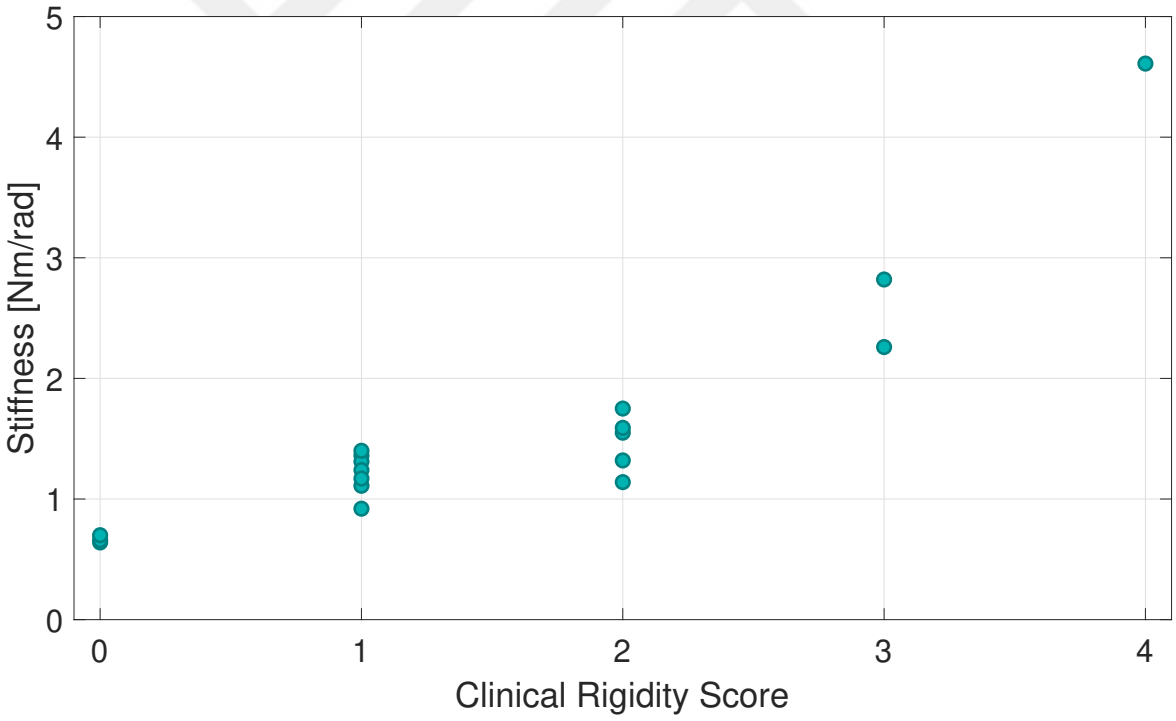


Figure 4.3. Scatter plot of stiffness values according to CRSs.

One-way ANOVA analysis was performed to find out whether the mean values of CRS groups are statistically significant or not. Subsequently, pairwise comparisons of the groups were analyzed with Tukey's range test.

One-way ANOVA test assumes that the data follows a normal distribution (normality) and that groups have the same variance (homoscedasticity). The homoscedasticity of the groups was tested with Barlett's method with a significance level of 0.05. The p-value of the test was found as 0.100 which means that we have enough evidence to conclude that group variances are equal. After checking normality and homoscedasticity of the CRS groups, one-way ANOVA and Tukey's post-hoc tests were performed. The p-value was found as 0 after the one-way ANOVA analysis that indicates the mean differences between the CRS groups are statistically significant ($\alpha = 0.05$). The results of pairwise comparison of the groups are given in Table 4.4.

Table 4.4. Table of Tukey's simultaneous tests for difference of group means.

Pairwise Comparisons	**Difference of Means**	**SE of Difference**	**95 %CI**	**T-Value**	**Adjusted p-value**
CRS - 1 vs. CRS - 0	0.55	0.14	(0.13; 0.97)	3.85	0.009
CRS - 2 vs. CRS - 0	0.80	0.15	(0.36; 1.25)	5.33	0.001
CRS - 3 vs. CRS - 0	1.87	0.19	(1.32; 2.43)	9.94	0.000
CRS - 2 vs. CRS - 1	0.25	0.12	(-0.10; 0.61)	2.10	0.203
CRS - 3 vs. CRS - 1	1.32	0.17	(0.84; 1.81)	8.00	0.000
CRS - 3 vs. CRS - 2	1.07	0.17	(0.56; 1.58)	6.19	0.000

Individual confidence level is 98.84%.

The group pairs 1 - 0, 2 - 0, 3 - 0, 3 - 1 and 3 - 2 are statistically significant among themselves ($p < 0.05$). On the other hand, CRS - 2 and CRS - 1 are not statistically significant ($p = 0.203$). The differences between the group means are plotted in Figure 4.4. If an interval bar in the plot contains zero, the corresponding group means are not statistically significant. Also box plots of the clinical rigidity groups are plotted in Figure 4.5.

The stiffness values were also grouped according to the condition of the trials they collected: activated, resting, on and off. Descriptive statistics about these groups are given in Table 4.5. First, in order to prove that the stiffness values of the "on" and "off" periods are statistically significant, OFF+NF and ON+NF, OFF+F and ON+F pairs were compared with Wilcoxon signed-rank test.

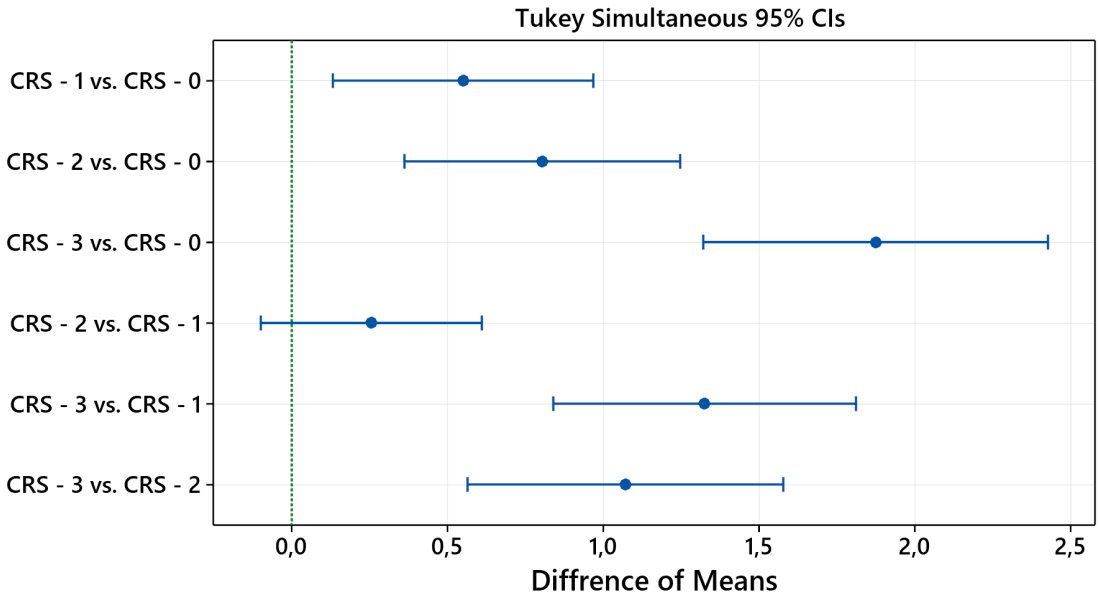


Figure 4.4. Interval bar plots of Tukey's HSD test results.

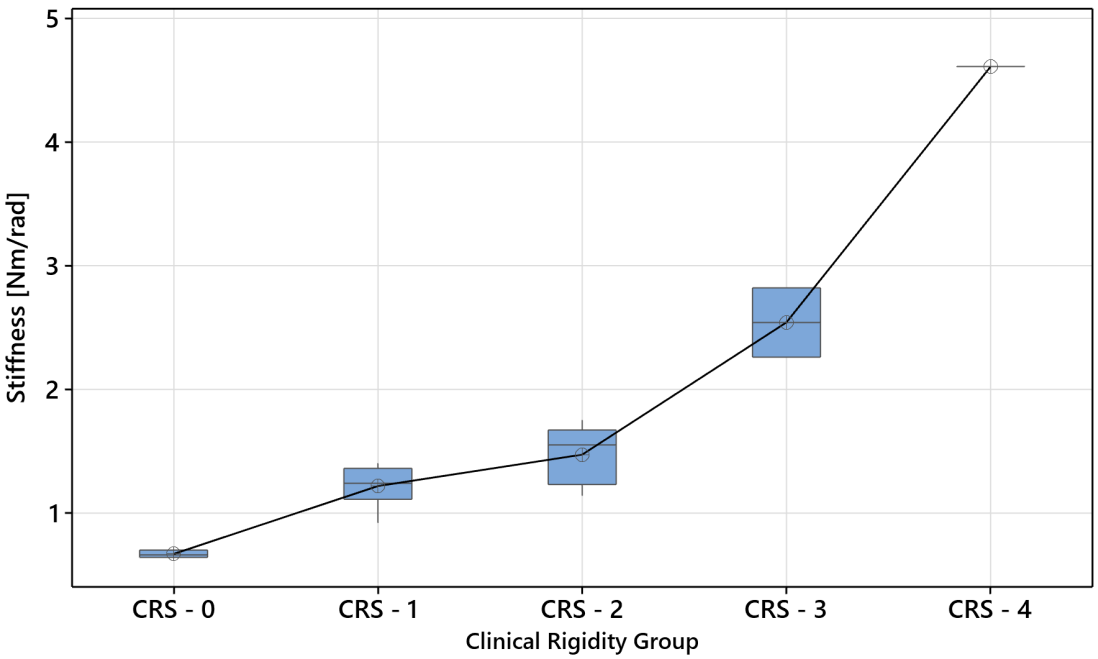


Figure 4.5. Box plots of clinical rigidity groups.

Table 4.5. Descriptive statistics about the clinical trials.

Group	N	Mean	SE Mean	St.Dev.	Min.	Q1	Median	Q3	Max
OFF+NF	9	1,87	0,39	1,18	0,66	1,23	1,55	2,29	4,61
ON+NF	9	1,19	0,16	0,48	0,64	0,81	1,17	1,35	2,26
OFF+F	9	2,98	1,07	3,20	1,20	1,46	1,59	3,40	11,21
ON+F	9	1,70	0,55	1,64	0,73	0,89	1,25	1,56	6,01

Two-sample t-test was not chosen because data sets violate the assumption of normality, the normality of the data sets were examined with Anderson-Darling test ($\alpha = 0.05$) and p-values of tests were found less than 0.05 for OFF+NF, OFF+F and ON+F which shows that the individual stiffness values of the these clinical trials are not normally distributed. Likewise, to prove that the stiffness values of the activated and rest conditions are statistically significant, OFF+NF and OFF+F, ON+NF and ON+F pairs were compared with each other by using Wilcoxon signed-rank test.

Results of pairwise comparisons are given in Table 4.6. The last row of the table contains the comparison of ON+NF, which is the trial where the lowest stiffness values are expected, and OFF+F, which is the trial where the highest stiffness values are expected.

Table 4.6. The median differences between clinical trials.

Group Pair	Groups Size	Median	Wilcoxon Statistic	p-value
OFF+NF and ON+NF	9	0.54	42	0.024
OFF+F and ON+F	9	0.86	44	0.013
OFF+F and OFF+NF	9	0.47	36	0.014
ON+F and ON+NF	9	0.13	40	0.044
ON+NF and OFF+F	9	1.05	45	0.009

The p-values in the last column of the table are less than to the significance level of 0.05. We can conclude that the differences between the clinical group medians are statistically significant. The boxplots and line plots of the on and off trials are given in Figure 4.6.

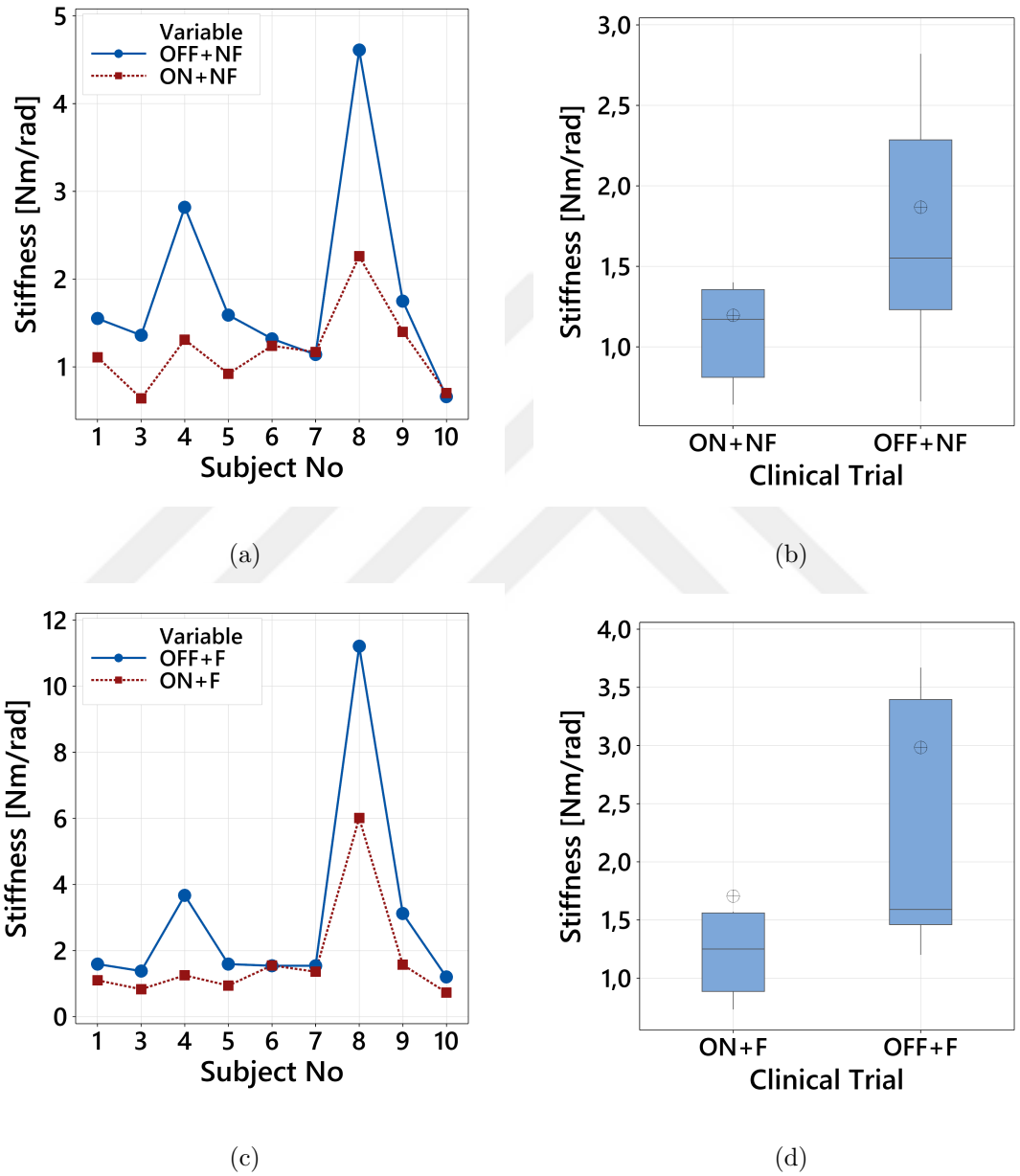


Figure 4.6. The stiffness difference between on and off conditions. (a) and (c) are the line plots of individual stiffness values, (b) and (d) are the boxplots of stiffness values.

As can be seen from Figure 4.6, the stiffness values in off condition are greater than the values in on periods, regardless of whether the patients are in the activate or resting conditions. However, stiffness values of the subjects 6, 7 and 10 did not differ. Similarly, the boxplots and line plots of the rest and activated trials are given in Figure 4.7. As can be seen from Figure 4.7, the stiffness values in the activated conditions are greater than the values in the rest conditions, regardless of whether the patients are in the on or off periods.

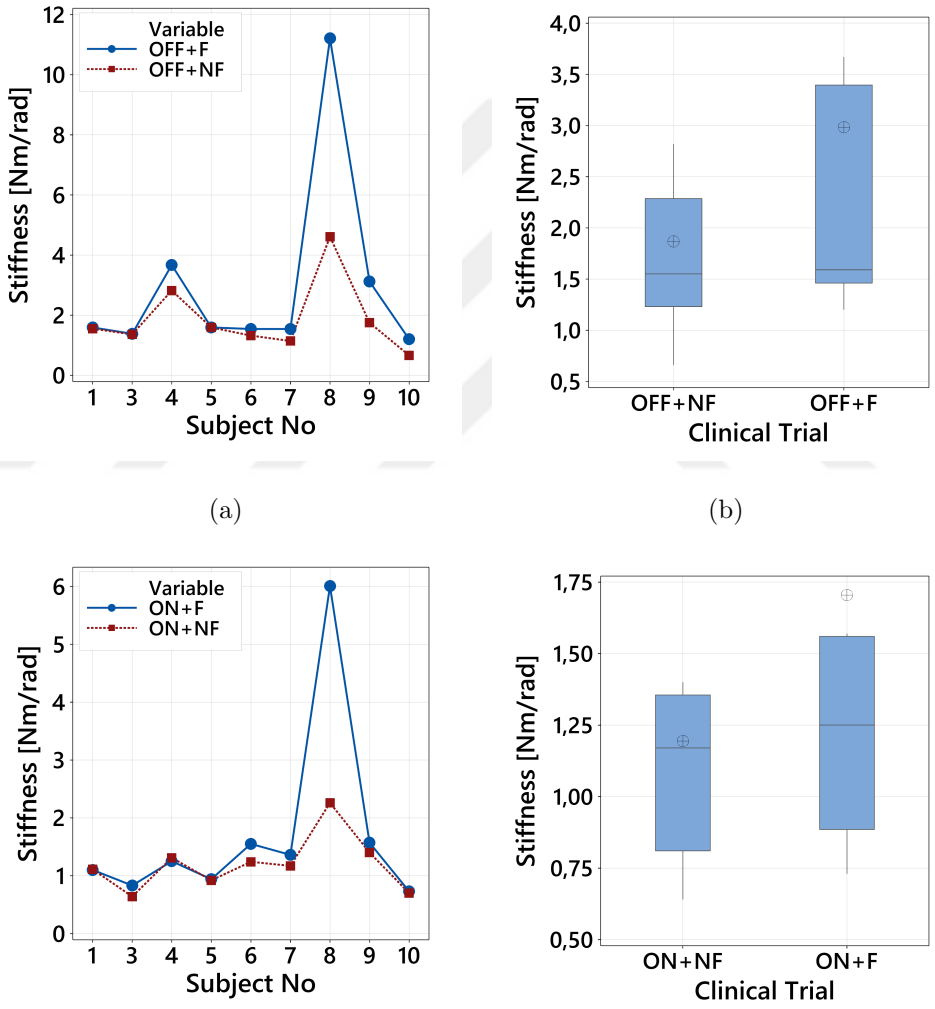
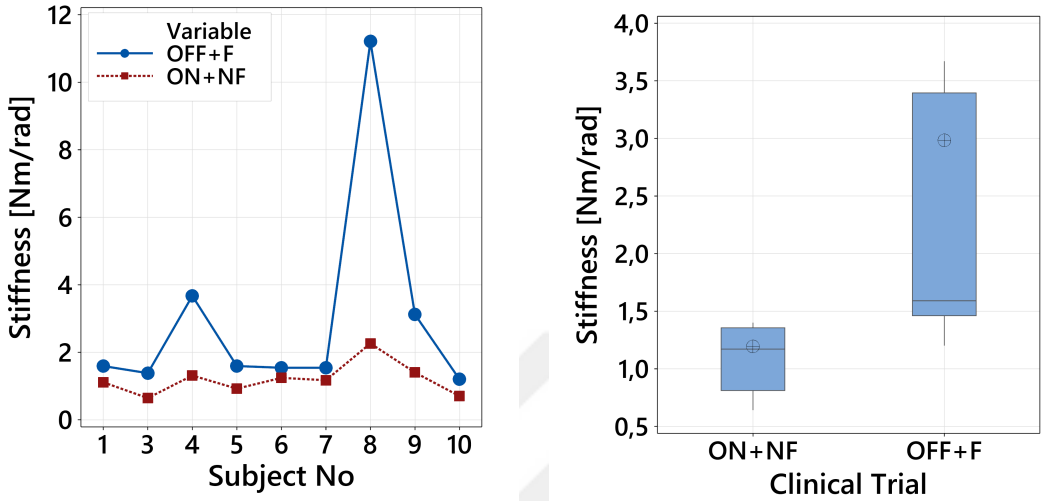


Figure 4.7. The graphical summary of the activated and rest trials. (a) and (c) are the line plots of individual stiffness values, (b) and (d) are the boxplots of the activated and rest trials.

The maximum stiffness difference is observed for comparison of the trials ON+NF and OFF+F in terms of the median difference (1.05 Nm/rad). The boxplots and line plots of the ON+NF and OFF+F comparison are given in Figure 4.8.



(a) (b)

Figure 4.8. The graphical summary of the comparison of two trials that the maximum stiffness differences are expected. (a) The line plots of individual stiffness values, (b) the boxplots of the compared groups.

Consequently, the stiffness values are more affected by on-off conditions rather than rest-activated conditions considering the results of the median differences between the trails.

Data sets collected from healthy subjects were also analyzed, descriptive statistics of the trials are given in Table 4.7 for both resting and active conditions. Clinical rigidity was observed in some participants as can be seen from the table. The stiffness values were classified into four groups and the group statistics were given in Table 4.8. The normality of the groups CRS - 0, CRS - 1 , R and A were tested with Anderson-Darling ($\alpha = 0.05$). The p-values of the tests were found as greater than the significance level, therefore it can be assumed that groups data follow a normal distribution. Subsequently, F-test was used to check that whether the groups are homoscedastic or not, the p-values of the tests found as greater than 0.05 which means

all variances are equal. After checking normality and homoscedasticity, two sample T-test was used to compare CRS - 0 and CRS - 1 assuming that the group variances are equal, the p-value of the test was found as 0.020 which means the mean values of the groups; CRS - 0 and CRS - 1, are statistically significant. The estimated difference between CRS - 0 and 1 was found as 0.11 Nm/rad with 95% confidence interval for difference (0.04 - 0.34).

Table 4.7. Descriptive statistics about the data collected from healthy subjects.

C. No.	Trial	N	CRS	Mean	S.E. Mean	St.Dev.	Min.	Q1.	Med.	Q3	Max.
1	NF	46	1	0,89	0,04	0,25	0,54	0,71	0,81	0,98	1,57
	F	80	*	0,96	0,03	0,26	0,47	0,79	0,92	1,11	1,96
2	NF	36	1	0,75	0,04	0,24	0,40	0,58	0,70	0,85	1,62
	F	72	*	0,73	0,02	0,18	0,38	0,59	0,70	0,85	1,22
3	NF	85	0	0,73	0,02	0,18	0,34	0,60	0,71	0,85	1,22
	F	105	*	0,61	0,02	0,17	0,30	0,49	0,58	0,71	1,22
4	NF	84	0	0,61	0,02	0,15	0,26	0,51	0,61	0,72	1,03
	F	86	*	1,07	0,04	0,35	0,42	0,82	1,00	1,25	2,05
5	NF	60	0	0,57	0,01	0,08	0,41	0,52	0,55	0,62	0,77
	F	63	*	0,61	0,02	0,12	0,37	0,53	0,60	0,69	1,01
6	NF	16	1	0,82	0,07	0,27	0,52	0,66	0,73	0,96	1,47
	F	56	*	0,88	0,08	0,58	0,16	0,54	0,72	1,10	4,08
7	NF	69	0	0,86	0,02	0,14	0,51	0,77	0,88	0,97	1,21
	F	68	*	0,86	0,02	0,19	0,57	0,72	0,81	0,93	1,43
8	NF	63	1	1,00	0,02	0,15	0,68	0,91	0,97	1,07	1,41
	F	62	*	1,08	0,02	0,15	0,70	0,97	1,08	1,20	1,34
9	NF	69	1	0,98	0,02	0,20	0,60	0,80	0,98	1,13	1,52
	F	58	*	1,09	0,04	0,30	0,57	0,87	1,01	1,29	1,81
10	NF	71	1	0,94	0,02	0,20	0,26	0,81	0,93	1,01	1,50
	F	90	*	0,97	0,02	0,19	0,64	0,86	0,94	1,09	1,67
11	NF	63	0	0,79	0,03	0,22	0,20	0,65	0,78	0,95	1,34
	F	58	*	0,83	0,02	0,18	0,46	0,69	0,83	0,94	1,36

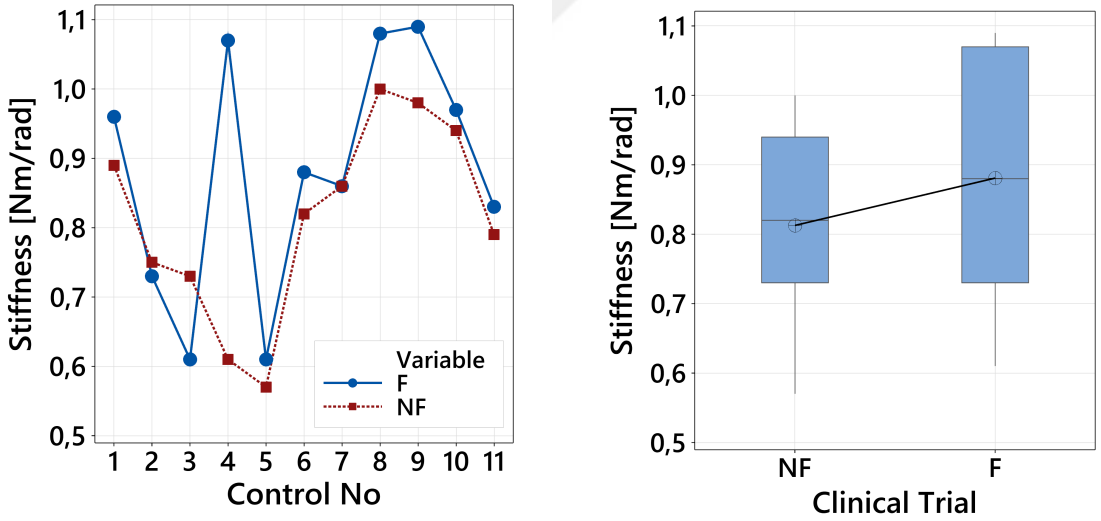
* In clinical practice, this maneuver is only used for differentiating CRS-0 from CRS-1.

In addition, the same test was used to compare the rest and activated conditions, the p-value was found as 0.326 which means the mean values of the groups are not statistically significant. The graphical summary of the rest and activated trials for the control groups are given in Figure 4.9.

Table 4.8. Descriptive statistics about the grouped stiffness values evaluated for control subjects.

Group	N	Mean	SE Mean	St.Dev.	Min.	Q1	Median	Q3	Max
CRS - 0	5	0.71	0.05	0.12	0.57	0.59	0.73	0.82	0.86
CRS - 1	6	0.90	0.04	0.10	0.75	0.80	0.92	0.98	1.00
NF	11	0.81	0.04	0.14	0.57	0.73	0.82	0.94	1.00
F	11	0.88	0.05	0.17	0.61	0.73	0.88	1.07	1.09

Finally, we compared PD patients with healthy individuals having no clinical rigidity sign (CRS - 0). One-way Anova and Dunnett's test were used in order to compare the mean stiffness values of the clinical rigidity groups. Normality assumption was checked in this section, previously. On the other hand, equal variance assumption was tested with Bartlett's method ($\alpha = 0.05$). The results of the Dunnett's test are given in Table 4.9.



(a) (b)

Figure 4.9. The graphical summary of the activated and rest trials of the control groups. (a) the line plots of the stiffness values of activated and rest trials, (b) the boxplot of the same trials.

The mean difference between the groups CRS - 0 and control is not statistically significant as expected. On the other hand, other comparisons seen in the table are statistically significant ($p < 0.05$). Interval plots of the group comparisons are given in the Figure 4.10. The boxplot of the clinical rigidity groups and control group is given in Figure 4.11.

Table 4.9. Table of Dunnett simultaneous tests: comparing group means with the control mean.

Pairwise Comparisons	Difference of Means	SE of Difference	95 %CI	T-Value	Adjusted p-value
Control - CRS – 0	-0.05	0.14	(-0.42; 0.33)	-0.33	0.99
Control - CRS – 1	0.50	0.11	(0.20; 0.81)	4.53	0.00
Control - CRS – 2	0.76	0.12	(0.43; 1.08)	6.31	0.00
Control - CRS – 3	1.83	0.16	(1.40; 2.26)	11.50	0.00

Individual confidence level is 98.52%.

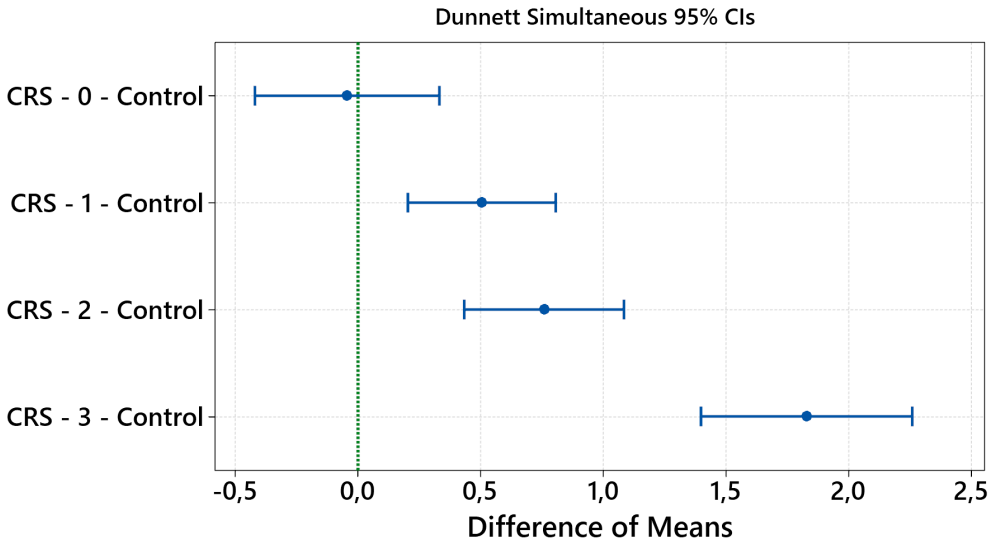


Figure 4.10. Interval plots of the control group and PD patients, control subjects who have the sign of rigidity were excluded from the control group.

Previously reported elastic stiffness values of the wrist and elbow were compared with our findings. The findings of Endo *et al.* [19] are given in Figure 4.12. Although, they found a positive correlation between UPDRS rigidity score and elastic stiffness, no

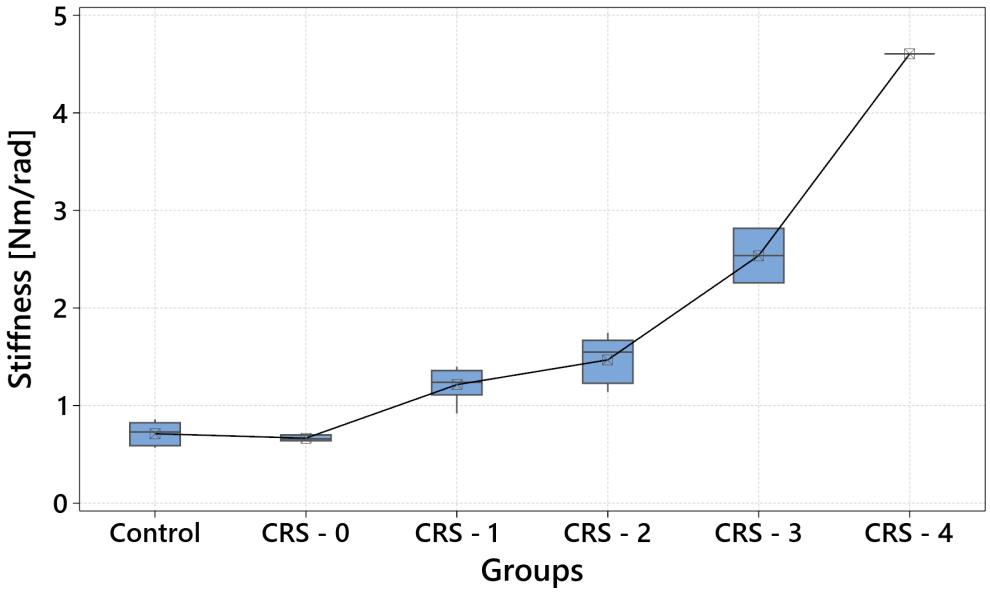


Figure 4.11. Box plots of the control group and PD patients, control subjects who have the sign of rigidity were excluded from the control group.

significant difference between the UPDRS 0 - 1, and UPDRS 3 - 4 groups was observed in extension and flexion. Park et al. tried to correlate wrist model parameters: viscosity and elastic stiffness, with UPDRS rigidity scores of the PD patients. The relationship of elastic component and UPDRS rigidity scores of PD patinets and healthy contols are given in Figure 4.13. As can be shown in Figure 4.13, UPDRS rigidity groups overlaps, especially groups 2 and 3.

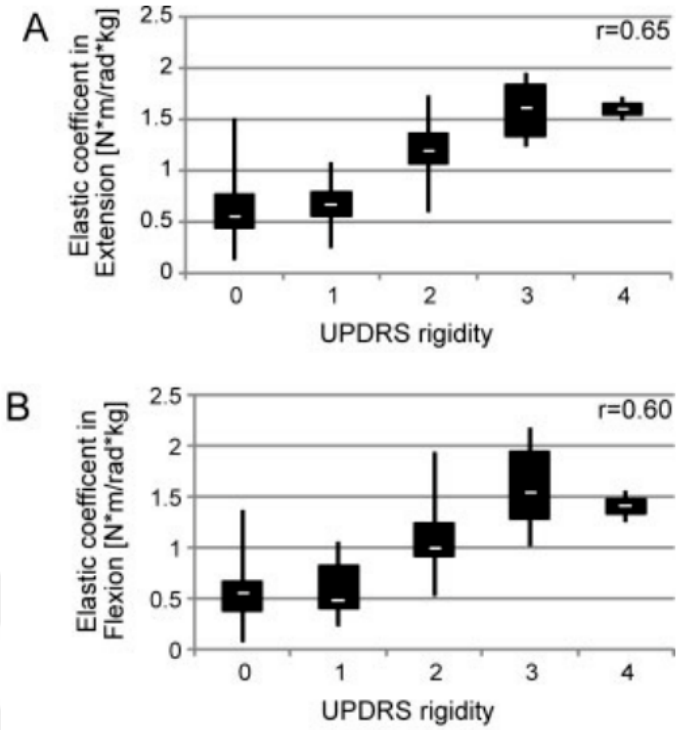


Figure 4.12. Measured elastic coefficients by Endo *et al.* [19], A: extension, B: flexion (reprinted from [19]).

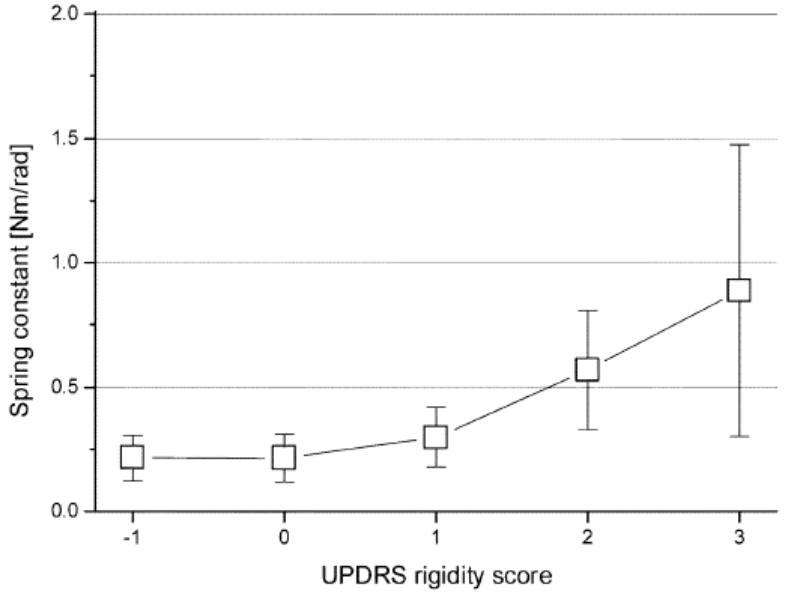


Figure 4.13. Relationship between elastic stiffness and UPDRS rigidity score. "-1" indicates healthy controls (reprinted from [17]).

5. CONCLUSION

In this study, a new method for objective assessment of wrist rigidity in PD patients has been introduced. The method requires a smartphone and an external deformable semi-conductive gadget to perform a rigidity measurement in a clinical environment. The manufacturing and calibration processes of the gadget have been presented. The method has been tested in clinical environment with both PD patients and healthy subjects. The elastic component of the adopted wrist model was used as an index of wrist rigidity. The results of the conducted experiments have shown that the method can assess the severity of wrist rigidity with respect to the UPDRS rigidity scale. The highest and lowest stiffness values in PD patients found as 11.21 Nm/rad and 0.64 Nm/rad, respectively. The results also have shown that performing a contralateral hand maneuver has an intensifying effect on the rigidity for PD patients; however, for healthy participants we do not have enough evidence to prove the same effect ($p > 0.05$). In addition, the withdrawal of the dopaminergic treatment and turning of the DBS system enhanced the wrist rigidity. The highest stiffness values were observed during the experiments when patients were in the off condition and performed a contralateral hand maneuver. On the other hand, the method failed in distinguishing the patients having clinical rigidity scores 1 and 2 ($p > 0.05$). The definition of the clinical rigidity scores 1 and 2 in the UPDRS are slight or detectable and mild, respectively. These neighbour rigidity scores might be hard to distinguish sometimes even for experienced neurologists. On the other hand, biased assessments of the neurologists may have caused a misclassification of the patients. The failure of the method may stemmed from these subjective and biased assessments. In addition, the deformable tip of the gadget does not have enough resolution to distinguish clinical rigidity scores 1 and 2. The conductive filler ratio of the gadget determines the stiffness of the gadget, this stiffness effects the resolution of the method.

5.1. Contributions and Originality

The originality of this method is provided by using a smartphone to assess wrist rigidity instead of using a servomotor, portable transducer with different sensors such as gyroscope and accelerometer or an electromyograph. One can prefer using portable transducers or gloves coated with motion sensors instead of using a smartphone with an extra deformable gadget; however, using smartphone offers extra options. Smartphones can be used to measure angle besides force and they can store rigidity values in its memory, or they can send these values to a remote server. This might help neurologists in tracking rigidity changes of patients over time. In addition, the application of the method is relatively easy-to-apply in the clinical environment and has sufficient accuracy comparing with the other methods in the literature. This study has not yet contributed to the literature as a publication; however, an invention disclosure form patent has been filed for the method and it is in review, currently.

5.2. Outlook and Future Work

The presented method also requires an extra gadget other than the phone to perform a rigidity assessment; however, the gadget is not an indispensable component of the method. The rigidity measurements can be performed without the gadget; however, we wanted to make the method more consistent and achieve high inter- and intra-rater reliabilities. The gadget might be eliminated from the method by just applying force to the phone screen with the right or left thumb of the person who performs the assessment by deploying some more complex algorithms and calibration processes. Due to limited time and number of participants to the experiments, we first want to demonstrate that the method can be used for assessing the wrist rigidity in PD patients. In addition, the application can be improved and updated for assessing other symptoms of PD. Although there are studies assessing motor symptoms of the disease other than rigidity in the literature, there is no comprehensive smartphone application, currently. A single comprehensive smartphone application that assesses multiple motor symptoms of the disease such as tremor, bradykinesia and rigidity can be developed in the future. In fact, such an application may even become a clinical standard.

REFERENCES

1. Parkinson, J., "An Essay on the Shaking Palsy", *The Journal of Neuropsychiatry and Clinical Neurosciences*, Vol. 14, No. 2, pp. 223–236, 2002.

2. Goetz, C. G., "The History of Parkinson's Disease: Early Clinical Descriptions and Neurological Therapies", *Cold Spring Harbor Perspectives in Medicine*, Vol. 1, No. 1, pp. a008862–a008862, 2011.

3. Guttman, M., S. J. Kish and Y. Furukawa, "Current concepts in the diagnosis and management of Parkinson's Disease", *CMAJ : Canadian Medical Association journal*, Vol. 168, No. 3, pp. 293–301, 2003.

4. Deuschl, G., P. Bain and M. Brin, "Consensus Statement of the Movement Disorder Society on Tremor", *Movement Disorders*, Vol. 13, No. S3, pp. 2–23, 1998.

5. Hoehn, M. M. and M. D. Yahr, "Parkinsonism: onset, progression, and mortality", *Neurology*, Vol. 17, No. 5, pp. 427–427, 1967.

6. Goetz, C. G., W. Poewe, O. Rascol, C. Sampaio, G. T. Stebbins, C. Counsell, N. Giladi, R. G. Holloway, C. G. Moore, G. K. Wenning, M. D. Yahr and L. Seidl, "Movement Disorder Society Task Force report on the Hoehn and Yahr staging scale: Status and recommendations The Movement Disorder Society Task Force on rating scales for Parkinson's disease", *Movement Disorders*, Vol. 19, No. 9, pp. 1020–1028, 2004.

7. Fahn S, Elton RL, UPDRS Program Members, "Unified Parkinson's disease rating scale", *Recent developments in Parkinson's disease*, Vol. 2, pp. 153–163, 1987.

8. Broussolle, E., P. Krack, S. Thobois, J. Xie-Brustolin, P. Pollak and C. G. Goetz, "Contribution of Jules Froment to the study of Parkinsonian rigidity", *Movement Disorders*, Vol. 22, No. 7, pp. 909–914, 2007.

9. Benabid, A. L., S. Chabardes, J. Mitrofanis and P. Pollak, "Deep brain stimulation of the subthalamic nucleus for the treatment of Parkinson's disease", *The Lancet Neurology*, Vol. 8, No. 1, pp. 67–81, 2009.

10. Matsumoto, K., F. Rossmann, T. H. Lin and I. S. Cooper, "Studies on induced exacerbation of Parkinsonian rigidity: The effect of contralateral voluntary activity", *Journal of Neurology, Neurosurgery and Psychiatry*, Vol. 26, No. 1, pp. 27–32, 1963.

11. Wright, V. and R. J. Johns, "Quantitative and qualitative analysis of joint stiffness in normal subjects and in patients with connective tissue diseases", *Annals of the Rheumatic Diseases*, Vol. 20, No. 1, pp. 36–46, 1961.

12. Mortimer, J. A. and D. D. Webster, "Evidence for a quantitative association between EMG stretch responses and Parkinsonian rigidity", *Brain Research*, Vol. 162, No. 1, pp. 169 – 173, 1979.

13. Teräväinen, H., J. K. Tsui, E. Mak and D. B. Calne, "Optimal Indices for Testing Parkinsonian Rigidity", *Canadian Journal of Neurological Sciences / Journal Canadien des Sciences Neurologiques*, Vol. 16, No. 2, p. 180–183, 1989.

14. Caligiuri, M. P., "Portable device for quantifying parkinsonian wrist rigidity", *Movement Disorders*, Vol. 9, No. 1, pp. 57–63, 1994.

15. Fung, V. S. C., J. A. Burne and J. G. L. Morris, "Objective quantification of resting and activated parkinsonian rigidity: A comparison of angular impulse and work scores", *Movement Disorders*, Vol. 15, No. 1, pp. 48–55, 2000.

16. Patrick, S., A. Denington, M. Gauthier, D. Gillard and A. Prochazka, "Quantification of the UPDRS rigidity scale", *IEEE Transactions on Neural Systems and Rehabilitation Engineering*, Vol. 9, No. 1, pp. 31–41, 2001.

17. Park, B. K., Y. Kwon, J.-W. Kim, J.-H. Lee, G.-M. Eom, S.-B. Koh, J.-H. Jun and

J. Hong, "Analysis of Viscoelastic Properties of Wrist Joint for Quantification of Parkinsonian Rigidity", *IEEE Transactions on Neural Systems and Rehabilitation Engineering*, Vol. 19, No. 2, pp. 167–176, 2011.

18. Charles, S. K. and N. Hogan, "Dynamics of wrist rotations", *Journal of Biomechanics*, Vol. 44, No. 4, pp. 614–621, 2011.

19. Endo, T., R. Okuno, M. Yokoe, K. Akazawa and S. Sakoda, "A novel method for systematic analysis of rigidity in Parkinson's disease", *Movement Disorders*, Vol. 24, No. 15, pp. 2218–2224, 2009.

20. Milette Greg, S. A., *Professional Android Sensor Programming*, John Wiley & Sons, New York, USA, 2012.

21. Züngör, G., *Assessment of Wrist Rigidity in Parkinson's Patients: A New Approach Based on Frequency Analysis*, Master's Thesis, Boğaziçi University, 2020.

APPENDIX A: TECHNICAL DRAWINGS

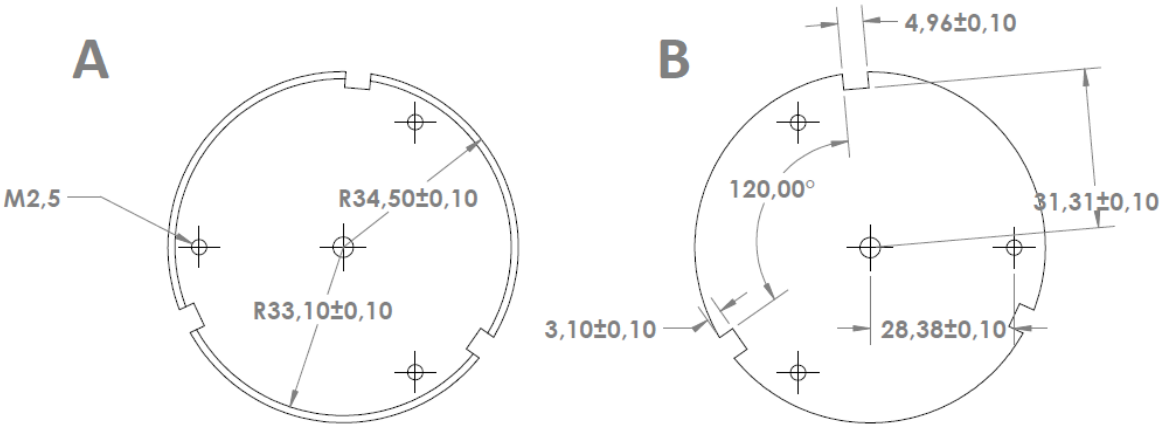


Figure A.1. The top cover of the gadget. A: bottom view, B: top view. All dimensions are in mm.

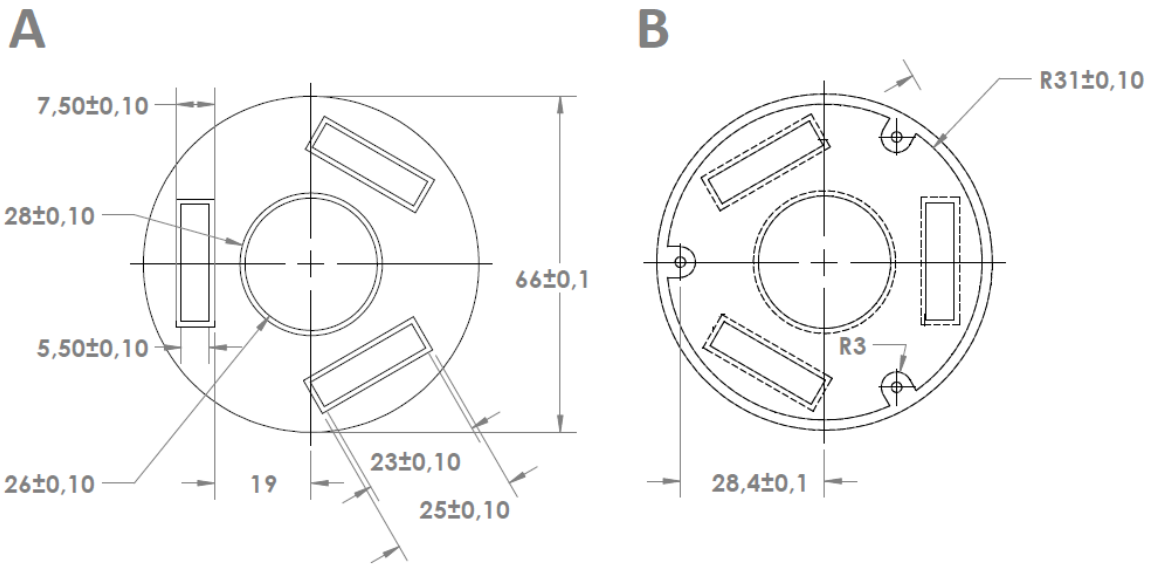


Figure A.2. The body of the gadget. A: bottom view, B: top view. All dimensions are in mm.

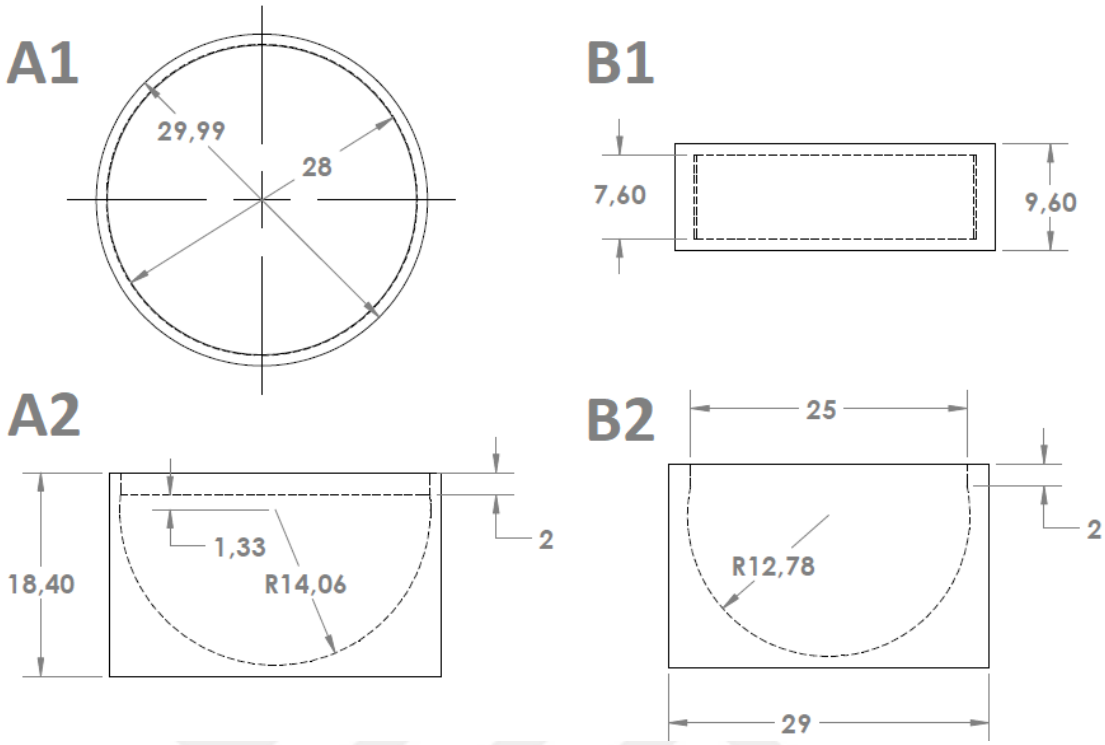
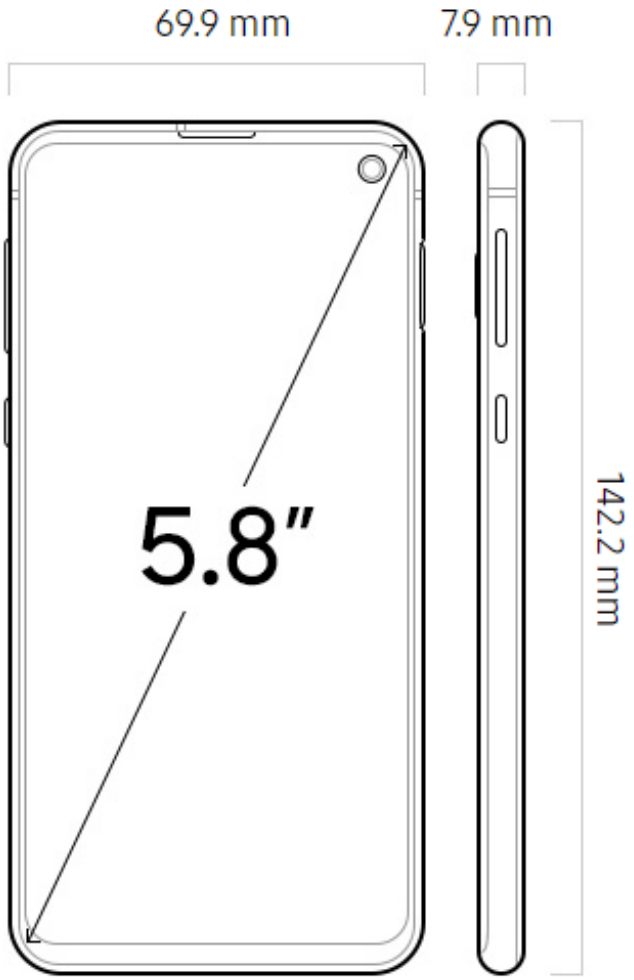


Figure A.3. The molds of the gadget tips. A1: top view of the mold used for the center tip, A2: side view, B1: top view of the molds used for the support tips, B: side view. All dimensions are in mm.



Galaxy S10e

Dimensions: 142.2 x 69.9 x 7.9 mm

Weight: 150 g

Figure A.4. Samsung s10e dimensions.

APPENDIX B: FORMS

“Parkinson Hastalarında El Bileğindeki Rijiditenin Cihaz Aracılığı ile Objektif Olarak Ölçülmesi” Çalışması Bilgilendirilmiş Gönüllü Olur Formu

Dr …… tarafından …… Üniversitesi Tıp Fakültesi Nöroloji A.D.’da tıbbi bir araştırma yapılacağı belirtilerek bu araştırma ile ilgili bilgiler bana aktarıldı. Bu bilgilerden sonra böyle bir araştırmaya “katılımcı” (denek) olarak davet edildim. Eğer bu araştırmaya katılırsam hekim ile aramda kalması gereken şahsi bilgilerimin gizliliğine bu araştırma sırasında büyük özen gösterileceğini biliyorum. Araştırma sonuçlarının eğitim ve bilimsel amaçlarla kullanımı sırasında kişisel bilgilerimin ihtimamla korunacağı konusunda bana yeterli güven verildi.

Çalışmanın yürütülmesi sırasında herhangi bir sebep göstermeden araştırmadan ayrılabilirim. Ayrıca tıbbi durumuma herhangi bir zarar verilmemesi koşuluyla araştırmacı tarafından araştırma dışı tutulabilirim. Araştırma için yapılacak harcamalarla ilgili herhangi bir ödeme yapmayacağım. Bana da bir ödeme yapılmayacaktır. Araştırma sırasında bir sağlık sorunu ile karşılaştığımda; herhangi bir saatte, hangi araştırıcıya, hangi telefon ve adresten ulaşabileceğimi biliyorum.

Çalışma kapsamında; Parkinson hastalığı bulguları açısından hekim tarafından muayene edileceğim, akıllı cep telefonunu elimde tutarken, bilek hareketlerimin çeşitli ölçümlerinin alınacağı, uygulamanın yaklaşık 2 saat süreceği söylendi.

Bu çalışmaya katılmak zorunda değilim. Araştırmaya katılmam konusunda zorlayıcı bir davranışla karşılaşmadım. Eğer katılmayı reddedersem, bu durumun tıbbi bakımıma ve hekim ile olan ilişkime herhangi bir zarar getirmeyeceğini de biliyorum. Bana yapılan tüm açıklamaları ayrıntılarıyla anladım. Kendi başıma belli bir düşünme süresi sonunda adı geçen bu araştırmada “katılımcı” (denek) olarak yer alma kararını aldım. Bu konuda yapılan daveti büyük bir memnuniyet ve gönüllülük içerisinde kabul ediyorum. İmzalı bu form kağıdının bir kopyası bana verilecektir.

Ben ……., bu çalışma bana açıklandı. Çalışma ile ilgili tüm sorulara tatmin edici yanıtlar aldım. Çalışmaya kendi rızamla gönüllü olarak katılmayı kabul ediyorum.

Katılımcı Adı Soyadı: Tarih İmza

Dr. Adı Soyadı: Tarih İmza

Tanıklık Eden Kurum Yetkilisi Adı Soyadı: Tarih İmza

Figure B.1. The informed consent form.

“Parkinson Hastalarında El Bileğindeki Rijiditenin Objektif Olarak Ölçülmesi” Çalışması Hasta Takip Formu

Hastanın adı:
Yaş:
Cinsiyet:
Eğitim:
El tercihi:
Meslek:
Hastalık Başlangıç Tarihi:
Özgeçmiş:

Kullanılan ilaçlar:

Hoehn Yahr:

Hipomimi varlığı:

Hipofoni varlığı:

	SAĞ		SOL	
	ÜST	ALT	ÜST	ALT
Bradikinezi				
İstirahat tremoru				
Çekme testi:				
Rijidite				

SAĞ EL BİLEĞİ	SOL EL BİLEĞİ
0: Normal: Rijidite yok. 1: Silik: Sadece aktivasyon manevrasıyla rijidite var. 2: Hafif: Aktivasyon manevrası olmadan rijidite var; ancak hareketin tamamı kolayca yapılıyor. 3: Orta: Aktivasyon manevrası olmadan rijidite var, hareketin tamamı eforla yapılıyor. 4: Şiddetli: Aktivasyon manevrası olmadan rijidite var, hareketin tamamı yapılamıyor.	0: Normal: Rijidite yok. 1: Silik: Sadece aktivasyon manevrasıyla rijidite var. 2: Hafif: Aktivasyon manevrası olmadan rijidite var; ancak hareketin tamamı kolayca yapılıyor. 3: Orta: Aktivasyon manevrası olmadan rijidite var, hareketin tamamı eforla yapılıyor. 4: Şiddetli: Aktivasyon manevrası olmadan rijidite var, hareketin tamamı yapılamıyor.
Sağ el bileği cihaz rijidite ölçümü	Sol el bileği cihaz rijidite ölçümü

Figure B.2. The patient follow-up form.